國立臺灣師範大學生命科學系博士論文

果蠅血管收縮素轉化酵素在心臟功能分析

Cardiac function analysis of angiotensin-converting enzyme-related (ACER) in *Drosophila melanogaster*

研 究 生：廖芳足
Fang-Tsu Liao

指導教授：蘇銘燦 博士
Ming-Tsan Su

中華民國 102 年 7 月

Content

Abstract

Studies have established the necessity of the angiotensin-converting enzyme-related (*Acer*) gene for heart morphogenesis in *Drosophila*. Nevertheless, the physiology of ACER has yet to be understood comprehensively. Herein, we used RNA interference and *Acer* mutants to down-regulate the expression of *Acer* in *Drosophila* heart and applied swept source optical coherence tomography to assess whether ACER is required for cardiac function in living adult flies. We showed that several contractile parameters of *Drosophila* heart, including heart rate, end-diastolic area, end-systolic area, percent fractional shortening, arrhythmicity index, and stress-induced cardiac performance, are age dependent and decline significantly when *Acer* is down-regulated. Moreover, the lifespans of *Acer* knock-down and mutant flies were significantly shorter than those of wild type control flies. Furthermore, to increase the expression of *Acer* for ACER deficient mutants, that phenotype of heart function resembled to the control. Thus, we posit that ACER, the *Drosophila* orthologue of mammalian angiotensin-converting enzyme 2, is essential for both heart physiology and longevity in animals. Because mammalian angiotensin-converting enzyme 2 controls many cardiovascular physiological features and is implicated in cardiomyopathies, our finding that *Acer* plays conserved roles in genetically tractable animals will pave the way to uncovering the genetic pathway that controls the renin-angiotensin system.

Key word: Drosophila, angiotensin-converting enzyme-related, swept source optical coherence tomography, heart function

摘　要

先前的研究已提出 Angiotensin-converting enzyme-related (*Acer*) 基因為果蠅心臟構造發育所需，不過 ACER 的生理功能並尚未被完全瞭解，有鑒於此，我們採用果蠅 RNA 干擾株和突變株來降低或提高 *Acer* 基因在果蠅心臟表現，並使用 Swept Source Optical Coherence Tomography (SS-OCT)光學同調斷層攝影技術來評估 ACER 是否為活的成蟲果蠅心臟功能所需，我們提出一系列依不同年齡的果蠅心臟收縮參數包括：心跳率(heart rate; HR), 心臟舒張末期面積(end-diastolic area; EDA), 心臟收縮末期面積(end-systolic area; ESA), 收縮分率(percent fractional shortening; %FS) , 心律不整率(arrhythmia index ;AI)和壓力所誘發心臟效能的影響。當 *Acer* 降調時果蠅隨著年齡增加而心臟功能顯著降低，此外，*Acer* 基因抑制和突變果蠅株的壽命也明顯地比野生型對照組果蠅低，並且用轉殖 *Acer* 的基因療法提高 *Acer* 表現量後，果蠅 *Acer* 突變株所造成的心臟功能衰竭症狀可接近於對照組，因此我們斷定哺乳動物其血管收縮素轉換酵素 2（Angiotensin-converting enzyme 2; ACE2）的果蠅同源基因 *Acer* 為心臟功能和壽命延長所需，因此哺乳動物的 ACE2 控制許多心血管的生理特性並涉及心臟的病理變化，本研究發現 *Acer* 運用於基因易操弄的動物模式將助於瞭解控制腎素-血管收縮素系統（Renin-angiotensin system; RAS）未知之基因路徑。

關鍵字：果蠅、血管收縮素轉化酵素、光學同調斷層攝影、心臟功能

General Introduction

The renin-angiotensin system (RAS) is an important regulator of blood pressure homeostasis, in which the protease renin cleaves angiotensinogen into angiotensin I (Ang I), which is then cleaved by angiotensin-converting enzyme (ACE) into angiotensin II (Ang II), causing blood vessel contraction and hypertension (Santos, Krieger et al. 2012). ACE2 has introduced further complexities into the canonical RAS signal cascade, as the major biologically active product of ACE2 hydrolyzes Ang II to form Ang-(1–7), thereby counterbalancing ACE activity (Donoghue, Hsieh et al. 2000, Tipnis, Hooper et al. 2000), which plays an important role in the development of cardiovascular disease. Research has led to the conclusion that the key point of ACE2 is to regulate blood pressure homeostasis (reviewed in (Keidar, Strizevsky et al. 2007, Wang, Bodiga et al. 2012, Burrell, Harrap et al. 2013).

ACE, the first member of the ACE family, is a well-known starting component of RAS that regulates blood pressure. ACE/ACE1 (EC 3.4.15.1, dipeptidyl dipeptidase A) was the first member of the M2 family discovered. It has a zinc metallopeptidase functional domain in the both N-terminal and C-terminal. ACE removes the C-terminal dipeptide of Ang I to generate Ang II as a strong vasoconstrictor and hydrolyzes Ang-(1–9) to produce Ang-(1–7) after ACE2 cleaves Ang I in the RAS system (Lambert, Yarski et al. 2005, Raizada and Ferreira 2007). 11 is mainly expressed in the lung, including vascular endothelial cells,

epithelial kidney cells, and testicular Leydig cells. Increased cardiac ACE does not trigger but augments cardiac hypertrophy (Tian, Hansen et al. 2004). Two subtypes of receptor Ang II-type 1 and Ang II-type 2 counteract the effect. The type 1 receptor is primarily involved in vasoconstriction (Touyz 2003), cell proliferation (Schelling, Fischer et al. 1991), vascular remodeling in hypertrophy by cardiac fibroblasts (Lijnen, Petrov et al. 2001, Vaughan 2001), renal tubular sodium reabsorption, inflammatory responses (Touyz 2003), and oxidative stress via biding to the active Ang II peptide. The type 2 receptor functions in fetal tissue growth and development, tissue remodeling after injury, and cardiac and vascular wound healing (Horiuchi, Lehtonen et al. 1999, Levy 2005). ACE inhibitors have demonstrated effectiveness in the treatment of hypertension, congestive heart failure, and renal disease in clinical trials, and their main mechanism of action is the blocking of Ang II effects.

More recently, another member of the family, ACE2, was discovered and determined to be a homologue of ACE (Vickers, Hales et al. 2002). ACE2 has nearly 40% amino acid sequence similarity with ACE. Unlike ACE, ACE2 preferentially removes a C-terminal hydrophobic or basic amino acid that contains a potential 17-amino acid N-terminal signal peptide and a putative 22-amino acid C-terminal membrane anchor. It also contains a conserved zinc metalloprotease consensus sequence (and a conserved glutamine residue that is predicted to serve as a third zinc ligand). ACE2 converts Ang I to the nonapeptide Ang-(1–9) (Donoghue,

Hsieh et al. 2000) or Ang II to Ang-(1–7) (Keidar, Kaplan et al. 2007). ACE2 directly regulates cardiac function in mammals. For instance, Ang II converted by ACE2 is a potent blood vessel constrictor. Ang-(1–9) has no effect on blood vessels but can be converted by ACE2 to a shorter peptide, Ang-(1-7), which is a blood vessel dilator in RAS (Boehm and Nabel 2002, Crackower, Sarao et al. 2002). Crackower et al. have shown that *ACE2* is highly expressed in kidney, testis, and heart. The expression levels in colon, small intestine, and ovary are moderate on northern blot analyses, demonstrating that *ACE2* maps to a defined quantitative trait locus on the X chromosome in three rat models of hypertension (Crackower, Sarao et al. 2002).

Targeted disruption of *ACE2* in mice results in a severe cardiac contractility defect with slight wall thinning and increased chamber dimensions. Genetic ablation of *ACE* on a*n ACE2* mutant background completely rescues the cardiac phenotype. ACE2 counteracts the aortic constriction effects of pressure overload mediated by Ang II; however, cardiac hypertrophy and dilatation occur with disrupted ACE2 and lead to heart failure in the short term (Yamamoto, Ohishi et al. 2006). In animal models o*f ACE2* overexpression, *ACE2* transgenic mice have a high incidence of sudden death with increased expression of cardiac ACE2; they also display severe, progressive conduction and rhythm disturbances with sustained ventricular tachycardia and terminal ventricular (Donoghue, Wakimoto et al. 2003). Overexpression of *ACE2* mRNA in

the cardiac tissue of Sprague-Dawley rats protects against the cardiac hypertrophy and myocardiac fibrosis induced by Ang II infusion (Huentelman, Grobe et al. 2005).

Invertebrate ACE, *Ance* (*Drosophila* angiotensin converting enzyme), *Ance2*, *Ance3*, *Ance4*, *Ance5* and *Acer* are provided with conserve (Houard, Williams et al. 1998). The *Ance* express in the amnioserosa, midgut during embryogenesis and that high levels are present in midgut, salivary gland and moderately high express in heart, hindgut and fat body of adult (Rusch and Levine 1997, Chintapalli, Wang et al. 2007). Heterozygous *Ance* causes male's sterility, homozygous *Ance* die at larva development, has unobvious phenotype abnormality. Biochemical study finds the Ang Ⅰ be converted to Ang Ⅱ by purification *Ance* of embryo, ACE inhibitor inhibits the enzyme activity (Williams, Danilov et al. 1996, Siviter, Nachman et al. 2002, Kim, Shin et al. 2003). The *Ance* still not verify the physiological functions of heart. The DNA sequences of *Ance2*, *Ance3*, *Ance4* and *Ance5* have highly conservation with *Ance*, but don't possess the active domain of metallopeptidase. The four genes exhibit membranous or secretory protein (Coates, Isaac et al. 2000), which contain N-terminal signal peptide. The genetic expressional position and function have vague, there have high conservation with peptidase sequence, but belong to process inactive non-peptidase, that were discovered in C. elegans, mouse and human genome(Huang, Sexton et al. 2003).

ACE-related (*Acer*) is a *Drosophila* homologue of ACE2 that is similar to the N-terminal metalloprotease of human ACE (Taylor, Coates et al. 1996). *Acer* exhibits enzyme activity through specificity of enzyme substrate and inhibitor (Isaac, Siviter et al. 2000). It is expressed in the embryo and pupa (Quan, Mita et al. 2001), specifically in the embryonic dorsal vessel of *Drosophila*. At later stages, high levels of *Acer* messenger RNA (mRNA) are present in fat body, hemolymph, and adult heart (Chintapalli, Wang et al. 2007, Arrese and Soulages 2010, Roma, Bueno et al. 2010). The *Acer* is disrupted reportedly results in severe defects of heart morphogenesis (Crackower, Sarao et al. 2002). Consequently, ACER has likely functions in *Drosophila* heart.. Studies have found that *Acer* is a maternal gene expressed in cardiac-related tissues including cardiac and cardiac precursor cells during embryo development. The *Acer* heart enhancer regulates ACER in myocardial cells and contains the binding sites of Tin (Tinman) protein (Lin 2004). Additionally, flies lacking ACER display increased activity during scotophase and reduction in nighttime sleep and greater sleep fragmentation (Carhan, Tang et al. 2011).

Drosophila is an excellent model of cardiovascular disease (Bier and Bodmer 2004, Wolf, Amrein et al. 2006, Nishimura, Ocorr et al. 2011, Diop and Bodmer 2012, Qian and Bodmer 2012). It has many advantages

as a model for human disease—for instances, it requires only simple genetic manipulation, has abundant research resources in Flybase, has a short lifecycle, and is easy to be maintained. Most important, 74% of disease-related genes in humans have homologs in *Drosophila*. Recently, many technologies have emerged for the assessment of cardiac function in *Drosophila*: electric pacing stress (Wessells and Bodmer 2004, Wessells, Fitzgerald et al. 2004), multielectrode array systems (Ocorr, Reeves et al. 2007), optical coherence tomography (OCT) (Wolf, Amrein et al. 2006), semi-automatic optical heartbeat analysis (Ocorr, Fink et al. 2009), atomic force microscopy (Kaushik, Fuhrmann et al. 2011), and multiple sensor electrocardiography (Slama 2012). The *Drosophila* model is expected to play important roles in the elucidation of the pathogenesis of human cardiovascular diseases.

Given the preceding evidence, I conducted researches with the following hypotheses and specific aims:

1. The Tin regulates the expression of *Acer* directly.

2. To establish a model with the semiautomatic and rapid quantification swept technique of source OCT (SS-OCT) imaging with wild-type flies.

3. To observe cardiac contractile parameters of manipulated *Acer* mutated by empolying an SS-OCT technique.

4. ACER flies with knockdown, deletion, overexpression, and rescue display cardiac performance under stress.

5. To investigate how the loss or function (LOF) and the gain of function (GOF) ACER flies affects longevity.

Chapter I. The Tin regulated directly the expression of Acer

1. Introduction

The renin-angiotensin-aldosterone system (RAAS) plays an important hormone rule in regulating arterial pressure and body fluid homeostasis of mammals. The system preserves blood osmosis and bold pressure homeostasis to regulate electrode, PH and body fluid by the filtration, resorption and excretion of the kidney. High blood osmosis stimulated antidiuretic hormone (ADH) excretion of the pituitary gland, the ADH raises resorption of water, reduces urine excretion then decreases blood osmosis (Ferreira and Santos 2005, Kurdi, De Mello et al. 2005, Leckie 2005). When blood pressure and blood volume is low, the juxtaglomerular cells in the kidneys secrete renin then hydrolyze angiotensinogen released by the liver to angiotensin Ⅰ (Ang Ⅰ), which converted to angiotensin Ⅱ (Ang Ⅱ) the enzyme angiotensin converting enzyme (ACE) found in the lungs. Ang II increases blood pressure by constricts the arteriole and stimulates the secretion of the hormone aldosterone to resorb the sodium and water. Blood pressure decreases by the process inhibition, that is the common therapy method for control hypertension (Ferrario, Jessup et al. 2005, Ferrario, Jessup et al. 2005, Karram, Abbasi et al. 2005, Keidar, Kaplan et al. 2007). The ACE2 of ACE homologue be discovered, ACE2 cleaves a single residue from Ang II to generate Ang 1-7, which reduces blood pressure by vasodilatation

(Riviere, Michaud et al. 2005, Keidar, Kaplan et al. 2007). Study finds that *ACE2* KO mice raises Ang II and reduces contractible function of heart (Crackower, Sarao et al. 2002).

The one of *Drosophila* homologue of ACE is called *Ance*. *Ance* exhibits enzyme activity similar to that of mammalian ACE. *Ance* is expressed mainly in the aminoserosa of *Drosophila* embryos and in germ cells and accessory glands of adult males (Tatei, Cai et al. 1995, Clark, Eisen et al. 2007). Even though the *Ance* of *Drosophila* moderately high express in heart, hindgut and fat body of adult. Expression profiles suggest that the function of *Ance* is mainly in germ cell morphogenesis.

The *Drosophila* homologue of ACE2 is ACER. The *Drosophila* embryo was used as a model for dynamic analysis of development using RNA in situ hybridization. *Acer* mRNA appears momentarily during the initial stage of embryo development and is apparently a maternal gene. Then ACER is expressed in amnioserosa and the dorsal mesoderm at stage 11, and expression continues to stage 14. As the amnioserosa progressively disappears, ACER appears clearly in cardiac precursor cells. ACER is expressed in cardiac cells only between stage 15 and late embryonic development and is restricted in cardiac cells at stage 16 (Lin 2004). At the dorsal vessel crossover at the dorsal midline, *Acer* mRNA is expressed in the 4 cardiac cells of each segment but not in pericardial cells. The other studys mention that *Acer* mRNA is found in the developing dorsal vessel (heart) during embryogenesis as well as the high

levels present in heart, hemolymph and fat body of adult (Taylor, Coates et al. 1996, Chintapalli, Wang et al. 2007, Arrese and Soulages 2010, Roma, Bueno et al. 2010). Lin (2004) has speculated that ACER plays an important role in the development of fly heart. Moreover, *Acer* mutant flies have a phenotype of cardiac cell deletion (Crackower, Sarao et al. 2002). Therefore, ACER can be inferred to be cell autonomous on fly cardiac development. The *Acer* heart enhancer contained upstream and an *Acer* gene intron reported by Lin (2004) suggest that green fluorescent protein of *Acer* heart enhancer expression is similar to that of cardiac tissue on in situ hybridization. Furthermore, we found that ACER expression highly overlapped with that of Tin during embryonic development. ACER clearly expressed the 4 cells of each segment expressed by after stage 16.

Previous studies have described *Acer* deletion phenotypes in cardiac cells of *Acer* p-element embryos (Crackower, Sarao et al. 2002). Clearly, ACER is essential for heart development in *Drosophila*.

The interaction and regulation of NK2, GATA and T-box transcription factors are required during cardiogenesis. Tin (Tinman) is an NK-2 homeobox transcription factor (Kim and Nirenberg 1989), as an Nkx2-5 of the mammalian, it is required for the development of mesoderm and the formation of heart (Azpiazu and Frasch 1993, Bodmer 1993). The Tin is crucial rule for Initiation of the heart specification, and ensues the genetic cascade during early cardiogenesis. The downstream

targets of *tin* have been mentioned, including the homeobox genes *even-skipped* (*eve*) and *ladybird* (*lb*) in heart progenitors (Bodmer, Jan et al. 1990, Azpiazu and Frasch 1993); the cardiac differentiation gene *β3 tubulin* (Kremser, Gajewski et al. 1999), *mef-2 gene* (Gajewski, Kim et al. 1997), *Hand* gene (Han, Yi et al. 2006); *seven-up* gene (Ryan, Hendren et al. 2007) and *Dorsocross T-box* genes in formation of ostial cell (Reim and Frasch 2005); zinc finger protein U-shaped as a negative transcriptional regulator (Tokusumi, Russell et al. 2007); cardiac expression of the *Drosophila sulphonylurea receptor* (*dSUR*) gene by *tin* gene and co-expression of the GATA genes *pannier* functionally interacts in an embryogenesis process (Akasaka, Klinedinst et al. 2006); the Toll enhancer is regulated by both Tin and Doc (Wang, Tao et al. 2005). Thus, it is confirmed that Tin is required for heart development genes. Tin protein expression within that four of six cardial and pericardial cell in each symmetrical segment of dorsal vessel (Cripps and Olson 2002). Therefore, *Acer* and *tin* likely have an upstream/downstream relationship.

2. Material and Methods

2.1 Fly stocks and genetics

All fly stocks and genetic crosses were maintained on standard yeast-glucose medium at 25°C. The *Acer*-en1 pGL3 *Acer*-enhancer1

DNA sequence was generated from *Acer* 1-4-4 and pH-Stinger via PCR using a pair of primers: *Acer* 1-5′ TAAAGTTATATGCTCGTGCG and *Acer* 1-3′ AAGTGCACCGAAATTAGGTA (Lin 2004). Amplified DNA was cloned first into a pCRII vector using TOPO TA cloning technology (Invitrogen), then into a pGL3 vector for luciferase expression by the enhancer. The pCRII and pGL3 vectors were deleted via restriction enzyme *Hind* III and *Xbo* I. The digested DNA fragment was blunt-ended with T4 DNA polymerase and re-ligated with T4 DNA ligase. The construct was confirmed via restriction enzyme BstN1 digestion and sequenced. *Acer*-en1 pGL3 Tin binding site-directed mutagenesis was generated using 2 pairs of primers: T1m-S 5′-ATTGTATCATTCTACCAGGAACCGTTTTTTATAA-3′, T1m-A 3′-TAACATAGTAAGATGGTCCTTGGCAAAAAATATT-5′, T2m-S 5′-AGAAATAGCTTATCCCAGGGACATTTATCTGTGG-3′, and T2m-A 3′-TCTTTATCGAATAGGGTCCCTGTAAATAGACACC-5′. The *Acer*-en1 pH-Stinger Tin binding site-directed mutagenesis was generated from *Acer*-en1 pGL3 mutagenesis via PCR using a pair of primers: *Acer*-U 1-5′ CACCTAAAGTTATATGCTCGTGCG and *Acer* 1-3′ AAGTGCACCGAAATTAGGTA. Amplified DNA was first into a pENTR/D TOPO vector (Invitrogen) and confirmed via sequencing and then transferred into a pH-Stinger vector, which was confirmed using restriction enzyme BstN1 and BstB1 digestion.

2.2 Site-directed mutagenesis

Site-directed mutagenesis was carried out using QuikChange™ XL Site-Directed Mutagenesis Kits (Cat. No. 200517, Stratagene). The reaction was carried out in a final volume of 25 μL, including 2.5 μL of 10× reaction buffer, 10 ng of template DNA, 62.5 ng of sense and antisense primers, 50 μM deoxyribonucleotide triphosphates, 1.5 μL of Quick Solution, and 0.5 μL of Pfu turbo DNA polymerase. The reaction was temperature cycled with the following conditions: 2 cycles of denaturation at 95°C for 1 minute, 18 reaction cycles comprising denaturation at 95°C for 50 seconds, annealing at 60°C for 50 seconds, and elongation at 68°C for 12 minutes, followed by elongation at 68°C for 7 minutes. After cycling, the reaction was cooled, and 0.5 μL of *Dpn*I (10 U/μL) was added to digest the parental DNA template at 37°C for 1 hour. Then, 5 μL of the reaction was used to transform the competent cells, and the site-directed mutant DNA was extracted from the cultured clones and sequenced.

2.3 Drosophila Schneider's 2 (S2) cell cultivation and transfection with cellfectin (Invitrogen #10362-010)

S2 cells (obtained from C. T. Chien) were maintained in Schneider's *Drosophila* medium (GIBCO) supplemented with 10% fetal bovine serum (FBS, GIBCO) at 25°C. S2 cell transfection was carried out as follows: 0.3 μg DNA was placed into 10 μL serum-free medium (SFM)

as solution A, and 1 μL Cellfectin was added to 10 μL SFM, which was inverted 5–10 times as solution B. Solutions A and B were mixed in a 96-well plate and incubated at 25°C for 30 minutes. At the time of DNA-Cellfectin complexation, a cell suspension of an appropriate number (1×10^5) per well was simultaneously prepared in 80 μL SFM without antibiotics and incubated at 25°C for 4 hours. The cells were spun down at 1,200 RPM for 5 minutes, resuspended with 4 mL 10% FBS complete medium, and incubated at 25°C at least 24 hours for transfected cell activity and 48 hours for luciferase reporter assay.

2.4 Luciferase reporter assay (Promega)

Transfected cells were harvested after 48 hours, and the cell pellet and lysis buffer reaction was centrifuged. Ten microliters of lysates was then added (1) to 50 μL LARH substrate (in vitro mutagenesis kit, Lot # 25968101, Stratagene, La Jolla, CA) for firefly luciferase level determination or (2) to stop buffer for Renilla luciferase level determination. Dual luceriferase assay was carried out using a luminometer (Promega). Each reporter construct measured 3 times the ratio of the firefly luciferase to Renilla luciferase level.

2.5 Chromatin immunoprecipitation (ChIP) assay

Tinman cDNA (clone RE01329) from the *Drosophila* Genomics Resource Center was amplified using a pair of primers

(5′-CACCATGTTGCAGCACCATCAGCAG-3′;
5′-CATGTGCTGCATCTGTTGCTG-3′), inserted into a pENTR-Topo plasmid (Invitrogen), sequenced, and transferred to a pAWF plasmid containing Flag. S2 cells were maintained in Schneider's *Drosophila* medium (GIBCO Co.) supplemented with 10% FBS (GIBCO Co.) at 25°C. Then, 1×10^6 cells/mL S2 cells were disposed in FBS-free Schneider's *Drosophila* medium and transfected via Fugene transfer reagent (Roche Applied Science) after culture for 16~24 hrs. A modified ChIP procedure **(**Upstate Millipore) was carried out as follows (Das, Ramachandran et al. 2004): Cells were washed twice with phosphate-buffered saline at room temperature and resuspended to approximately 2×10^7 cells/mL. Then 1% formaldehyde (final concentration) was added, and the cells were incubated with shaking at 37°C for 10 minutes (for cross-linked histones and DNA). The cells were then washed twice with phosphate-buffered saline containing protease inhibitor. The cell pellet was collected after centrifugation at 2,000 RPM for 4 minutes. The cells were resuspended in lysis buffer (sodium dodecyl sulfate + protease inhibitor) via gentle mixing. The reaction took place on ice for 10 minutes. Then, DNA was broken into 200~2,000 bp segments using a Microson^{TM} Ultrasonic cell disruptor on ice 24 times for 30 seconds at intervals of 1 minute, 30 seconds at a power output setting of 5–6. The crude nuclear extract was collected via microcentrifugation at 13,000 RPM for 10 minutes at 4°C and transferred to a 2-mL

microcentrifuge tube. The protein concentration of the supernatant was determined at an optical density of 260 nm.

The supernatant was then divided into 3 tubes labeled A, B, and C. The A tube was the positive control with directly extracted DNA. The B tube was the negative control and contained no antibody. The C tube was the experimental group contains antibody. The immunoprecipitation step was continued in the B and C tubes. First, 75 μL protein was treated with agarose/salmon sperm DNA blocking for 1 hour to remove nonspecific protein. The protein was then microcentrifuged at 3,000 RPM for 3 minutes at 4°C. The supernatant was transferred to a new microcentrifuge tube. To the C tube was added 10 μL anti-flag M2 (Sigma). The B and C tubes were incubated overnight at 4°C on a rotator and then 60 μg protein A agarose/salmon sperm DNA was added and mixed at 4°C on a rotator for 1 hour to combine the protein A agarose and the antibody completely. The tubes were microcentrifuged at 2,000 RPM for 2 minutes at 4°C to remove the supernatant. The precipitate was washed several times with low-salt, high-salt, and LiCl buffers, and then the protein A agarose and the antibody were separated using 0.1M $NaHCO_3$ and 1% sodium dodecyl sulfate solution at 25°C on a rotator for 30 minutes.

Twenty μL of 5M NaCl was added to reverse cross-linked DNA and protein in an incubating tube in a 67°C water bath that was mixed occasionally for more than 4 hours. The protein in each tube was decomposed with 2 μL proteinase K. To isolate the DNA, we extracted

supernatant once with 500 μL phenol/chloroform/isoamyl alcohol (25:24:1) and precipitated the DNA with 500 μL isopropanol. The precipitate was washed several times with 75% alcohol and air-dried. The DNA was dissolved with double-distilled water and stored at –20°C. PCR was carried out in a volume of 20 μL including 2 μL of 10× reaction buffer, 2 μL of template DNA, 2 μL of both sense and antisense primers (Tin binding site I primer: *Acer* 1-5′ TAAAGTTATATGCTCGTGCG, *Acer* 1-2-3′ TGCATTATCGGCGGGTTAGC; Tin binding site II primer: *Acer* 2-5′ AACTGGCTTGGTATTGGCGG, *Acer* 1-3′ AAGTGCACCGAAATTAGGTA), 2 μL deoxyribonucleotide triphosphates, 0.1 μL of Taq polymerase, and 10 μL double-distilled water. The reaction was temperature cycled with the following conditions: 1 cycle of denaturation at 95°C for 2 minutes, 35 reaction cycles comprising denaturation at 95°C for 30 seconds, annealing at 46°C, and 15 seconds for Tin binding at site I and annealing at 45°C, and 15 seconds for Tin binding at site II, and elongation at 72°C for 50 seconds, followed by elongation at 72°C for 7 minutes. The results of the reaction were checked by 1.5% agarose gel electrophoresis.

2.6 Statistical analyses

Statistical analyses were performed using SPSS (version 14.0, SPSS Inc.). A p value of <0.05 was considered statistically significant. The relative differences between 2 groups were compared using the Student's t-test: ***, $p < 0.001$; **, $p < 0.01$; *, $p < 0.05$.

3. Results

We found 2 Tin binding sites (T1, 5′-CACTTAA-3′; T2, 5′-CACTTGA) in DNA sequences of *Acer* heart enhancer. Thus, because Tin is a transcript protein, which is presumably bound on DNA sequences of *Acer* heart enhancer, we presume that *tin* is upstream of the *Acer* gene. We designed ChIP assays to test this hypothesis, and they showed that Tin binds to the T1 and T2 of *Acer* heart enhancer specifically in vivo, as assessed using S2 cell Tin protein (Fig. 1a). The relative activity of *Acer* heart enhancer was analyzed quantitatively. The assay was repeated 3 times with duplicated samples (Fig. 1b), and the data were analyzed with the Student's *t*-test and presented as average ± standard deviation (*, $p < 0.05$).

I investigated whether *Acer* heart enhancer promotes firefly luciferase reporter gene expression through *tin* expression, which could then prove that *Acer* is regulated by Tin. The position of *Acer* heart enhancer is from -188 to 1211 in a dotted line. The frames are exon1, exon2 and exon3, T1 binding site is before exon1, T2 binding site is after exon2. However, *Acer* heart enhancer cannot promote reporter gene expression in S2 cells. A 59-fold increase in the activity of firefly luciferase reporter gene expression was found in cotransfected *tin*-expressing plasmids (Fig. 2a). Mutation of the binding sites of Tin (T1m, 5′-CCAGGAA-3′; T2m, 5′-CCAGGGA-3′) was carried out through site-directed mutagenesis. Firefly luciferase reporter assay of

Acer heart enhancer showed abnormal expression in S2 cells when 2 mutated Tin binding sites (T1m + T2m; see Fig. 2b) were present. For the reasons outlined above, we conclude that Tin directly regulates *Acer* in the cardiac cells of flies. Two Tin binding sites are required for the heart specific enhancer of *Acer*. That is to say, when Tin binds on Two Tin binding sites to make GFP expression. The eGFP reporter expresses under control of both enhancers T1+T2 and T1m+T2m in embryo of *Drosophila* (Figs.3a, 3b). Thus, Tin exerts its effects upstream of *Acer*.

4. Discussions

ACE2 of the mammalian ACEs family plays an important role in RAS, which maintains blood pressure homeostasis, and is found in high levels in the heart, where it is involved in cardiovascular contraction, heart remodeling, and hypertrophy (Burrell, Johnston et al. 2004, Warner, Smith et al. 2004). *ACE2* knockout mice lack cardiac contractility with age (Crackower, Sarao et al. 2002). *Acer* is a homologue of *ACE2*, the mRNA of which can be found in the dorsal vessel during embryogenesis (Taylor, Coates et al. 1996). Lin (2004) has manipulated *Acer* mRNA using in situ hybridization, and *Acer* heart enhancer expressed the similarity position of *tin* expressed, clarifying the *Acer* phenotype expressed in the heart and cardiac tissue related to the *Drosophila* embryogenesis period. ACER clearly contributes to the embryogenesis of the *Drosophila* heart. We carried out a luciferase reporter assay of the Tin

bound to various mutated *Acer* heart enhancer genes and performed ChIP, demonstrating that *Acer* is regulated directly by Tin protein, which is essential during *Drosophila* heart development. The defects in cardiac cells were observed in embryos of *Acer* mutated flies (Crackower, Sarao et al. 2002). Notably, *Acer* is a homologue of mammalian *ACE2*, which has no effect on cardiac development in mammals but increases angiotensin II levels and causes severe cardiac contractility deficiency when disrupted in mice. ACE2 is considered necessary for physiological functioning in mice. In addition, ACER is strongly expressed in fat tissue, head, and heart of adult *Drosophila* according to FlyAtlas Anatomical Expression Data (Chintapalli, Wang et al. 2007). Considering the above evidence and observation, we infer that ACER is involved the cardiac development of flies. We proved that Tin directly regulates *Acer* during embryogenesis. The above-mentioned studies and heart development gene-binding sites on *Acer* heart enhancer suggest that *Acer* is related to heart physiology. Tin is required for the diversification, differentiation, and post-embryonic maturation of cardiomyocytes, which regulates interactions with *seven-up, midline, Dorsocross*. Furthermore, Loss of Tin in larval and adult hearts severely endangers the structure and function from morphologically dorsal vessel, cardiac pacing and survival assay (Zaffran, Reim et al. 2006). Consequently, if Tin regulates the Acer gene, and then our conjecture that ACER has a influence in the heart function of *Drosophila*.

5. Figures

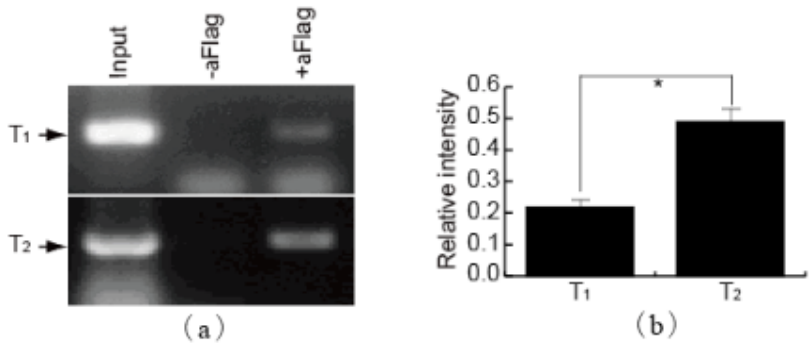

Fig. 1 Chromatin immunoprecipitation analysis shows that Tin binds to *Acer* enhancer. DNA from *Drosophila* Schneider's 2 (S2) cells was immunoprecipitated with Flag-tagged Tin. Tin binding sites on *Acer* en1 were amplified with PCR using specific primer sets and visualized on an agarose gel (a). Relative binding efficiencies were compared between Tin binding sites (T1 versus T2) using the Student's *t*-test (b). Data are expressed as mean + standard deviation (sd); *, $p < 0.05$ by Student's *t*-test.

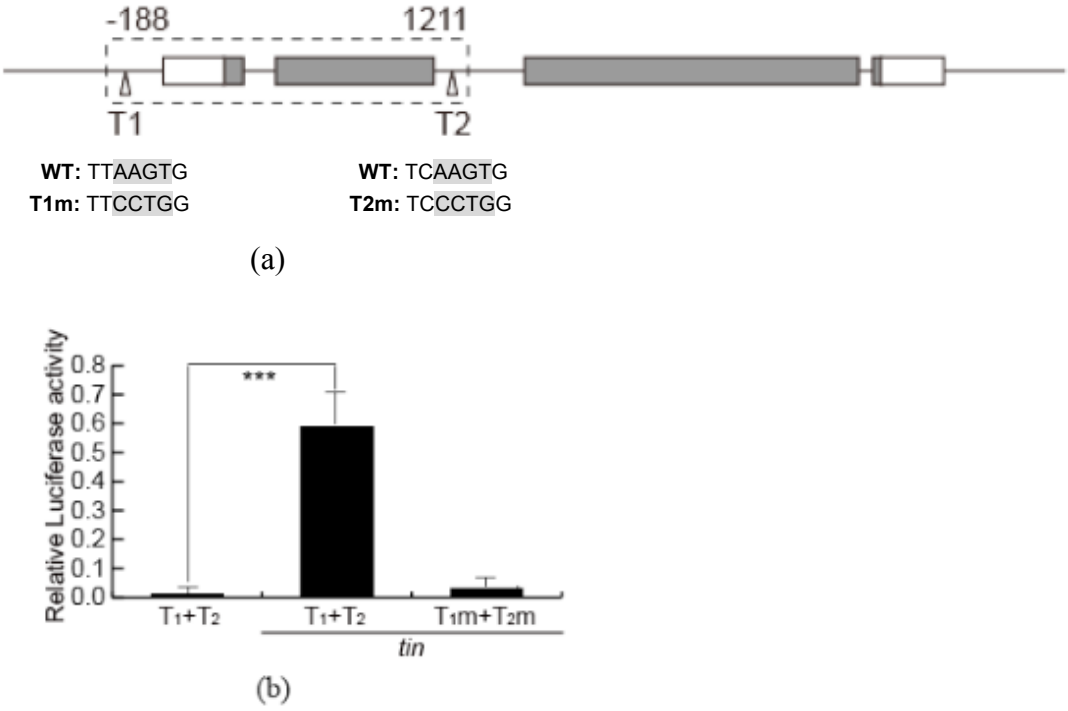

Fig. 2 Reporter assays show that Tin regulates the expression of *Acer*. (a) Tin binding sites were mutated as indicated (T1m and T2m). (b) Luciferase activities were analyzed 48 hours after transfection in S2 cells. Relative reporter activities were compared using Student's *t*-test. Data were expressed as mean + sd; *, $p < 0.05$).

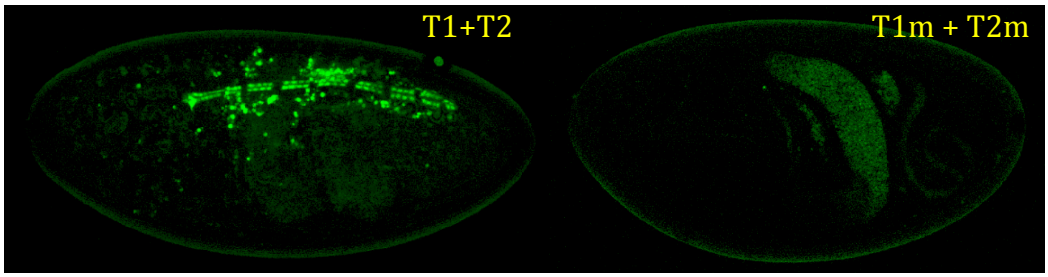

Fig. 3 Two Tin binding sites are required for the heart-specific enhancer of *Acer*. The expression of enhanced green fluorescent protein reporter under the control of various enhancers: (a) T1+T2; (b) T1m+T2m.

Chapter II. Semiautomatic and rapid quantification Swept technique of Source optical coherence tomography (SS-OCT) imaging

1. Introduction

Drosophila melanogaster has been a useful myocardial model for investigating human heart disease (Dulcis and Levine 2005, Monier, Astier et al. 2005, Akasaka, Klinedinst et al. 2006, Cammarato, Dambacher et al. 2008). Recently, many approaches have been proposed for assessing cardiac functions in *Drosophila*, such as using electropacing stress (Wessells and Bodmer 2004), optical coherence tomography (OCT) (Wolf, Amrein et al. 2006), multielectrode array systems (Ocorr, Reeves et al. 2007), semiautomatic optical heartbeat analysis (SOHA) (Ocorr, Fink et al. 2009), atomic force microscopy (Kaushik, Fuhrmann et al. 2011), and multiple sensor electrocardiography (Slama 2012).

Among these, OCT is a powerful tool for producing noncontact and noninvasive tomographic images of biological tissues. By measuring the echo time delay and the intensity of backscattered light from a specimen, OCT uses inherent differences in the index of refraction in tissue, rather than enhancement with dyes, to differentiate various tissue types. The extended imaging depth in the scattering medium enables OCT to successfully obtain in vivo images of the adult heart in *Drosophila* (Choma, Izatt et al. 2006, Wolf, Amrein et al. 2006, Bradu, Ma et al.

2009, Choma, Suter et al. 2010, Ma, Bradu et al. 2010, Tsai, Chang et al. 2011).

In previous studies using time-domain (TD) OCT, given the limitation of imaging speed, a number of heartbeat parameters have been obtained by manual counting; this involves tracking heart activity through a limited numbers of beats from M-mode OCT records (Choma, Izatt et al. 2006, Wolf, Amrein et al. 2006, Ma, Bradu et al. 2010). Since the recently developed frequency-swept lasers have improved sensitivity, making real-time B-mode and Doppler OCT imaging possible (Bradu, Ma et al. 2009, Choma, Suter et al. 2010, Tsai, Chang et al. 2011), high-throughput studies in *Drosophila* are now feasible. This requires an automated analyzing method for obtaining reliable measurements of dynamic heart function parameters in large samples or over a long period of time.

Therefore, in this study we proposed a rapid OCT-based method for obtaining cardiac parameters from adult flies. Our method is very useful, particularly in experiments with a large sample size. We adopted the random walker algorithm for semiautomatic cardiac chamber segmentation in B-mode OCT images. Random walker is a semiautomatic segmentation method based on graph theory by Leo Grady (Grady 2006); it requires that the user give some labels as input seed points for the cardiac chamber area and background. Greater detail of random walker segmentation will be described in the next section. First,

we created an initial set of seed points for the random walker algorithm on the first frame. In the next frame, the cross-sections of the heart tube are automatically segmented in a total of 2000 frames, and the size of the inner margin is represented by area for each *Drosophila*. Then, depending on the histogram distribution of the changing area during each heartbeat cycle, an optimum threshold can be chosen automatically by an iterative process (Ridler 1978). Thus, each heart period (HP) is subdivided into two meaningful sections, which are used to represent diastolic and systolic intervals (DI and SI), respectively. These two parameters are important for detailed heartbeat analysis.

The proposed method combines high-speed swept-source OCT (SS-OCT), for optical recording of beating hearts, with robust, semiautomatic analysis to rapidly detect and quantify, on a beat-to-beat basis, not only heart rate (HR) and HP but also DI and SI, and end-diastolic (EDA) and end-systolic area (ESA). These parameters can be used to determine dynamic parameters of heart function, including the arrhythmia index (AI) and percent fractional shortening (%FS). We also demonstrate age-related alterations observed in fly heart-function using this method. The convenience of the algorithm, and the relevance of our results to the human body, is also discussed.

2. Material and Methods

2.1 SS-OCT Imaging Technique

Drosophila (**w**^{1118}), used as wild-type strain, were maintained on regular yeast glucose media at 25°C. For image assessment, flies were first anesthetized by exposure to Fly Nap® (Carolina Biological Supply Company, Burlington, North Carolina). Flies were then immobilized on a plastic petri dish using jelly glue, with the dorsal side facing the OCT probe. For each time point, a group of 10 flies of different ages, including one-, three-, five-, and nine-week-old flies, were examined using the SS-OCT system (OCM1300SS; Thorlabs Inc., Newton, New Jersey).

Two-dimensional OCT images were obtained in the longitudinal direction to identify the conical chamber (CC) of the heart [Fig. 1(a)]. Then, the OCT image orientation was rotated by 90 degrees, such that the CC was acquired in the transverse plane of the *Drosophila*. Figure 1(b) and 1(c) shows representative transverse two-dimensional OCT images of the CC during diastole and systole, respectively, in a three-week-old wild-type *Drosophila*.

The SS-OCT system had a median wavelength of 1310 nm; an axial and transverse resolution of around 9 and 15 μm, respectively, in tissue; total power of 10 mW; and an A-scan rate of 16 kHz. For each measurement, around 2000 frames (each covering an area of 0.75 $\times$ 3 mm^2, corresponding to 128 $\times$ 512 pixels in the $Y - Z$ direction) was obtained at 92 frames per second.

2.2 Algorithm

We used a combination of two algorithms, written in Matlab, to automatically measure several heartbeat parameters in *Drosophila*. First, after contrast-enhancement of the original image, as shown in Fig. 1(d) and 1(e), an initial set of seed points are created by the user to indicate the inner margin (green point) of the heart chamber for the random walker algorithm. The red point is provided automatically by the algorithm, showing seed points at fixed positions to indicate the outer margin of the heart chamber and background. When the random walker moves from any pixel, it calculates a vector of probabilities, based on the correlation of both grey-level and distance for each pixel, to reach the specified seeds. As demonstrated in Fig. 1(f) and 1(g), the probability of every unlabeled point reaching the labeled points will be computed by this algorithm. Then, segmentation results can be obtained by performing thresholding on the probability map. The algorithm is summarized below, and more details can be found in Ref. (L. Grady, 2006).

Based on graph theory, a graph consists of a pair of points, G = *(V, E)*, with vertices set $v \in V$ and edge set $e \in E$. The weight of an edge *eij* has a weight *wij* between neighboring vertices *vi* and *vj*, with intensity *gi* and *gj*. The weighting function is given by

$$w_{ij} = \exp[-\beta(g_i - g_j)^2], \qquad (1)$$

where $\boldsymbol{\beta}$ is the constant for adjustment of *wij*. The discrete Dirichlet integral in a region χ is defined as

$$D[x] = \frac{1}{2} x^T L x, \tag{2}$$

where the Laplacian matrix L is defined as

$$L_{ij} = \begin{cases} d_i, & \text{if } i = j \\ -w_{ij}, & \text{if } v_i \text{ and } v_j \text{ are adjacent nodes,} \\ 0, & \text{otherwise} \end{cases} \tag{3}$$

in which *Lij* is indexed by vertices *vi* and *vj* and di is the degree of vertex *vi*. All pixels of the same region have a similar intensity, so that differentiating $D_{[\chi]}$ approximates zero. Given the labeled points χ_M, the unlabeled points χ_U can be solved by the discrete Dirichlet integral function.

$$D[x_U] = \frac{1}{2} [x_M^T x_U^T] \begin{bmatrix} L_M^T & B \\ B^T & L_U^T \end{bmatrix} \begin{bmatrix} x_M \\ x_U \end{bmatrix}. \tag{4}$$

The unlabeled area, $\chi_{\boldsymbol{U}}$, can be obtained by solving a sparse linear system in the differentiating $D[\chi_{\boldsymbol{U}}]$ as follows:

$$L_u x_U = -B^T X_M. \tag{5}$$

It is only necessary to position seeds on one frame; thereafter, the edges of the CC are automatically detected on every frame. Figure 2 demonstrates the area inside the boundary of the heart tube in 100 frames, where peak and trough positions represent EDA and ESA of the *Drosophila*. Here, we define FS = EDA − ESA⁄EDA, which represents the extent of change in the cardiac chamber area during systole; it can

provide an estimate of the contractility of the heart tube. HP is quantified as the time elapsed between the ends of two consecutive systoles (i.e., at the troughs of the filtered data, as indicated by the red line in Fig. 2). AI is defined as the standard deviation of HP, normalized to the median HP. This parameter provides quantitative representation of the arrhythmicity of the hearts of individual flies, which is useful for comparing groups of individuals.

Furthermore, in order to automatically estimate the length of diastole and systole, we adopted an automatic thresholding algorithm. First, we used the average value of the maximum and minimum areas on the histogram distribution during each heartbeat cycle as an initial estimate of the threshold **T**. Then, we partitioned the area in each HP into lower and higher groups, R1 and R2, using the threshold *T*. A new threshold is then created by calculating the mean values $\boldsymbol{\mu}_1$ and $\boldsymbol{\mu}_2$ of the two partitions, using the equation

$$T = \frac{1}{2}(\mu_1 + \mu_2). \qquad (6)$$

These three steps are repeated until the mean values, $\boldsymbol{\mu}_1$ and $\boldsymbol{\mu}_2$, do not change in successive iterations; the optimum threshold can then be chosen automatically as a result of this iterative process. In the process, each HP is subdivided into two meaningful regions; Figure 3 demonstrates two heartbeats, where SI is quantified as the interval during contraction (systole), which is, in turn, defined as the time occupied when

a cardiac area smaller than the mean μ_1 values of the lower group R1 are encountered. DI is then quantified as HP minus SI.

2.3 Statistical analyses

Statistical analyses were performed using SPSS (version 14.0, SPSS Inc.) A p value of <0.05 was considered statistically significant. The relative differences between 2 groups were compared using the Student's t-test: **, $p < 0.01$; *, $p < 0.05$.

3. Results

We first tested how inputting different numbers as seed points and in different regions could affect the probability distribution and the final segmentation. The representative result is shown in Fig. 4. For comparison, Fig. 4(a) shows the segmentation results manually measured by our expert. Figure 4(b) to 4(d) shows the segmentation results from inputting one, two, and three seed points, respectively, to indicate the inner margin. The right column of Figure 4 shows the enlarged images. For each image, we input seed points in 20 different randomly selected regions. Random walker segmentation resulted in the same mean area size (5419 μm2), irrespective of whether one, two, or three seed points were provided. The coefficients of variation (CV), which are defined as the standard deviation of area in percentage, normalized to the mean area,

for seed points provided in different regions were 0.13%, 0%, and 0% for inputting one, two, or three seed points, respectively. This indicates that the algorithm has very high precision in segmenting the *Drosophila* heart tube in OCT images.

Thereafter, we randomly selected 28 images (each with two seed points) and compared the size of the segmentation area with that obtained by manual segmentation. As shown in Fig. 5(a), the correlation coefficient between automated method and manual segmentation was 0.993, which demonstrated that the random walker algorithm is as accurate as the manual method in segmenting the *Drosophila* heart tube in OCT images.

In order to assess whether SI and DI detection, based on the automated thresholding algorithm, differs from that defined by manual interpretation by an expert user, manual measurements for DI and SI were obtained by the user adjusting the thresholds on the histogram distribution of a segmented area (e.g., in Fig. 2, where five representative DI and SI were measured for each fly). Using the contraction pattern provided by M-mode OCT as an objective assessment of heart wall motion, the user could then finely adjust the thresholds. We randomly selected four movies taken of one-, three-, five-, and nine-week-old flies and compared the manual measurements obtained in this manner with the output of our algorithm. Both DI and SI periods in the heart of *Drosophila* were measured manually and using the automated

thresholding algorithm. We evaluated the correlation of the manual and automated methods using canonical correlation, a statistical analysis method used to assess correlation of two sets of variables with more than one dimension (Hardoon, Szedmak et al. 2004). Figure 5(b) shows that the maximal canonical correlation found was 0.998, which indicates that the algorithm defined SI and DI as accurately as did manual measurements.

Figure 6 shows the M-mode contraction pattern, in which we can observe the phenomenon of prolonged relaxation time and irregular heart rhythms that occur with increasing age. In particular, flies in their ninth week of age displayed various forms of arrhythmia. Figures 7 to 10 summarize eight heartbeat parameters of male *Drosophila* $\mathbf{w}^{1118}$ derived and quantified by our automated algorithm, in their first, third, fifth, and ninth week, respectively. Data points represent the mean [± standard error of the mean (SEM)] for 10 files per datum point. Figure 7 shows a significant difference both in HP and HR between one- and three-week-old [analysis of variance (ANOVA), $P = 0.003$]], one- and five-week-old (ANOVA, $P = 0.001$) one- and nine-week-old (ANOVA, $P = 0.001$), three- and five-week-old (ANOVA, $P = 0.001$), and three- and nine week- old flies (ANOVA, $P = 0.001$). It was also quite clear from our data (Fig. 8) that DI in particular increased age, as compared to SI, with a significant difference in DI between three- and five-week-old flies (ANOVA, $P = 0.001$). Moreover, the variation in DI was more obvious

when comparing flies in their fifth and ninth weeks; this was consistent with Fig. 9, which shows the average AI, reflecting the age-related increase in arrhythmicity in flies (ANOVA, P = 0.007). However, the average size for ESA remains similar across age, while a small but statistically insignificant increase in EDA is shown in Fig. 10(a). For this reason, no significant decline in FS was observed, as shown in Fig. 10(b).

4. Discussions

Drosophila is an important model for investigating human heart diseases. Automated quantification of potentially relevant parameters from the model can replace labor-intensive manual work and generate more objective, accurate, and comprehensive metrics. A widely used approach for cardiac image analysis is to reduce complexity by using M-mode, which is the mono-dimensional projection of the image along a line. M-mode images are often used in echocardiography for the analysis of heart motion dynamics (Azevedo, Garcia-Fernandez et al. 1997). Previous methods (Choma, Izatt et al. 2006, Wolf, Amrein et al. 2006, Ma, Bradu et al. 2010) using M-mode OCT images were based on continuous in-depth scans in the midline of a fly's cardiac chamber over time; cardiac parameters, including HR, end-diastole diameters, and end-systole diameters, are manually measured and derived by averaging a few cardiac cycles during a normal, regular rhythm.

Automatic segmentation of cardiac M-mode images for identifying end-systole and end-diastole can be a challenge, although many methods have been proposed, such as gray level histograms, fuzzy set (Shapiro and Haralick 1985), Markov random field models (Tobias and Seara 2002), neural networks, binarization, morphology (Manay and Yezzi 2003), and many others. In these methods, borders are not well defined and the gray level is not uniform. Thus, Bertelli et al. (L. Bertelli et al. 2006) proposed a semi-automated method, which segments cardiac M-mode images by using a multiclassifier for computing cardiac parameters, such as the ratio between the diameters in end-diastolic and end-systole, or the ratio between diastolic and systolic durations. The required computational time for the process is about 25 s. Fink et al. (Fink, Callol-Massot et al. 2009) used a combination of two movement detection algorithms to track movement of heart edges from a semi-intact *Drosophila* heart. The user needs to adjust the thresholds and filters to finely tune the algorithm output, using M-mode as an objective assessment of heart wall movements.

In this study, instead of following the segmentation of cardiac M-mode images, cardiac parameters are measured on the basis of changes in the whole cross-sectional area of the cardiac chamber, rather than by measuring the brightness (i.e., gray level change) between the edge of the superior and inferior walls during mid-diastole and mid-systole in M-mode OCT images. Our proposed semi-automated segmentation

method, based on the random walker algorithm, can provide a unique, quality solution that is robust to weak/noisy object boundaries (Grady 2006). This is because, according to the theory of random walker segmentation, the performance of the algorithm depends on the weighting function in Eq. (1). Noise is usually considered to be a disturbance in a local region. This means that a region with noise has a greater intensity difference between adjacent pixels than a region without noise. The weighting function determines the influence of intensity difference between adjacent pixels. It decreases the effect of noise and increases the boundary effect. Further details and proofs can be found in Ref. (Grady 2006).

There are some other well-known segmentation methods, such as active contours or graph cuts. Segmentation based on active contouring (Sethian J. A.1999) has large time complexity and poses a local energy minimization problem, so that the method does not always present a correct solution, especially when segmenting images with a tortuous boundary or high noise levels. Figure 6 shows images with a markedly tortuous boundary and high noise level. Another well-known algorithm, graph cuts, (Boykov Y. Y. 2001) has been developed for automated and semi-automated segmentation. For automated segmentation, the performance of graph cuts is noticeably better than other methods. However, if an insufficient number of seeds are provided in the semi-automated segmentation, the "small cut" problem will decrease the

correctness of segmentation. Grady (Grady 2006) showed that random walker segmentation can cope with images with a tortuous boundary or high noise levels, has no local energy minimization problem, or "small cut" drawback, even if a small number of seeds are used. Our data confirmed that even in the presence of a degraded boundary, such as the cardiac tube of *Drosophila*, the algorithm could perform segmentation successfully (with a very high correlation to manual segmentation, R = 0.993). We also proved that when inputting more than two seed points, different regions of input would not affect the final segmentation result (CV = 0).

The automated thresholding algorithm is a simple and efficient statistical method for computing a threshold value automatically between two bimodal distributions, simply according to their mean value. In this study, we observed that the area distribution in diastole and systole followed a bimodal distribution. Thus, DI and SI, based on our algorithm, could be automatically and independently detected in each HP. This method was validated against manual interpretation by our expert, and the algorithm generated the SI and DI as accurately as did manual measurements (the methods were highly correlated, R=0.998). It should be noticed that there are periods of time when the speckle pattern is fixed on M-mode OCT images (Fig. 6); the rate of change of the heart segmented area at these times is zero, so that our automated thresholding algorithm detects "long" diastoles or systoles.

The quantitative heartbeat parameters measured using our proposed method show that as flies age, HP lengthens [Fig. 7(a)], resulting in an age-related decline in HR [which is the inverse of HP; Fig. 7(b)]. We also found that the age-dependent decrease in HR may be due to a disproportionate increase in DI, compared to SI, with age (Fig. 8). Moreover, the current algorithm not only measures HR but also quantitatively expresses the age-dependent increase of heartbeat arrhythmicity (i.e., AI), which may be due to large variations in DI associated with age, particularly when comparing flies in their fifth and ninth weeks of age (Fig. 9). These findings are consistent with results obtained with a movement detection algorithm by (Fink, Callol-Massot et al. 2009, Jolly, Xue et al. 2009). Ocorr et al. (Ocorr, Akasaka et al. 2007) also suggested that age-related cardiac dysfunction in the fly heart is due to a decrease in the efficacy of cardiac relaxation. Since age-dependent decreases in intrinsic HR, and increases in the incidence of AI, have also been documented in humans, (Jose, Stitt et al. 1970, Strobel, Epstein et al. 1999, Paternostro, Vignola et al. 2001, Wessells, Fitzgerald et al. 2004) our observation of the age-related changes in heart function of flies has correlates in humans.

Large variations existed in both EDA and ESA within the tested groups, which may be due to differences in size between flies; however, use of %FS can eliminate the effect of body size. (Fink, Callol-Massot et al. 2009) Have reported age-dependent decreases in FS. However, in our

study, no significant declines in %FS in fly hearts were observed with age, suggesting that muscle contractility remained similar across age. Previous studies using different cardiovascular stress methods to estimate end-systolic and end-diastolic dimensions also failed to detect significant alterations associated with aging. (Furberg, Psaty et al. 1994, Thom, Haase et al. 2006)

In this study, because the eight heartbeat parameters were automatically detected by manually positioning two seeds only on one frame, it only requires around 0.5 s to process a single fly (including a minimum of 100 cardiac cycles) with the proposed algorithm; this can be an efficient and useful approach for high-throughput gene-screening studies in *Drosophila*. Moreover, solving the solution of the random walker segmentation according to Eq. (5) is a linear system. Douglas et al. (Douglas, Romero et al. 1990) have demonstrated the design of analog circuit implementation from a linear system. This direct correspondence with analog electrical circuits opens the possibility for hardware implementation of the random walker segmentation algorithm. As the random walker algorithm can also operate in three dimensions, further research, combining faster SS-OCT scanning and more control of fly movement, may allow heart volume segmentation.

5. Conclusion

Here, we presented an algorithm for cardiac image segmentation with high precision and high accuracy, based on a small set of pre-labeled pixels. Furthermore, the technique we described here allows an optimum threshold to be chosen automatically as a result of an iterative process. By applying the semi-automated segmentation and auto-threshold algorithm, we established an easier and more accurate quantification method for measuring heart parameters in *Drosophila*. Both algorithms involve the use of a few empirical parameters and are expected to perform robustly in the presence of noise. Using our approach, we were able to show age-dependent changes in fly heart-function, including HP increases; disproportionate increases in DI and SI, increases in AI, and a similar %FS across age. The combination of high-speed and successive B-mode imaging features of SS-OCT gives this technique potential for automatically assessing large numbers of individuals over significant periods of time. OCT-based automatic and rapid quantification of cardiac parameters can facilitate future highthroughput studies in *Drosophila*.

6. Figures

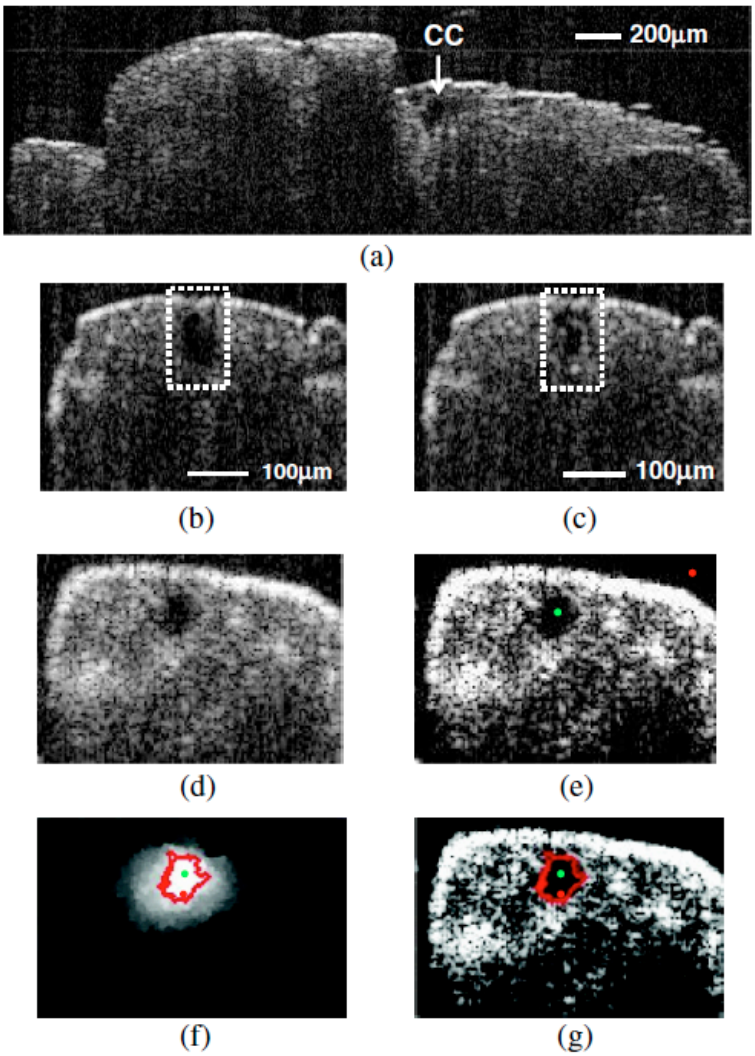

Fig. 1 Representative B-mode OCT images. The arrow shows the conical heart chamber (CC) (a) in longitudinal orientation and (b) and (c) in transverse orientation. The dorsal side is at the top of the images. Squares show the heart wall in the (b) diastolic and (c) systolic stages. Parts (d) and (e) show the process of implementation of the autosegmentation algorithm. (d) Original image. (e) Enhanced image. (f) Related probability distribution. (g) Red circle indicates the heart segmentation result.

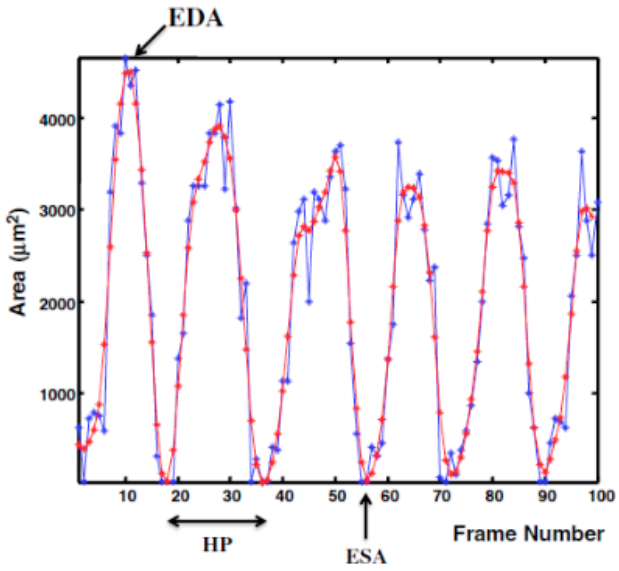

Fig. 2 Change in area inside the segmented boundary of the heart tube during heart contraction. Blue: original data, red: filtered data for determining positions of troughs only. Heart period (HP) is the time between 2 troughs. EDA, end-diastolic area; ESA end-systolic area.

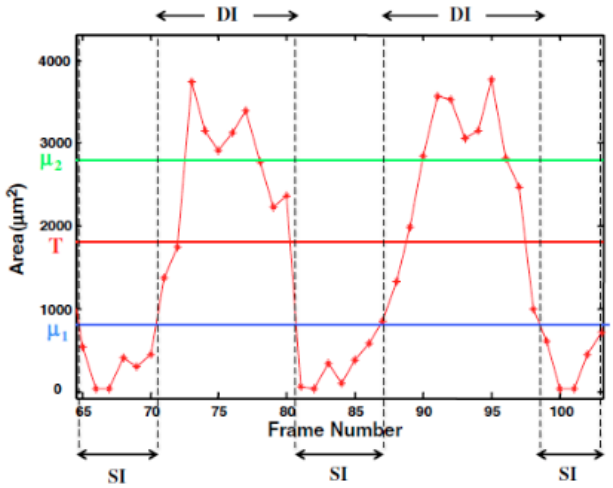

Fig.3 Change in area inside the segmented boundary of the heart tube in two heart periods. Horizontal lines represent the automatic thresholding result. T, optimum threshold; $\boldsymbol{\mu_2}$, the average of the upper group; $\boldsymbol{\mu_1}$, the average of the lower group.

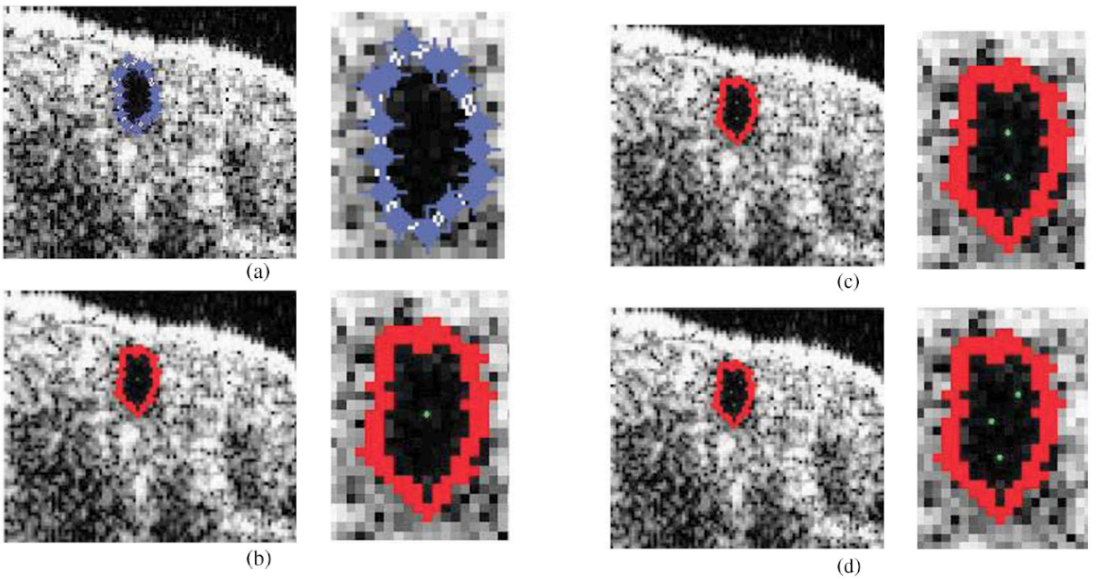

Fig.4 Segmentation results from (a) manual segmentation by our expert, (b) to (d) semi-automated method, by inputting one, two, and three seed points, respectively. Right column shows the enlarged images.

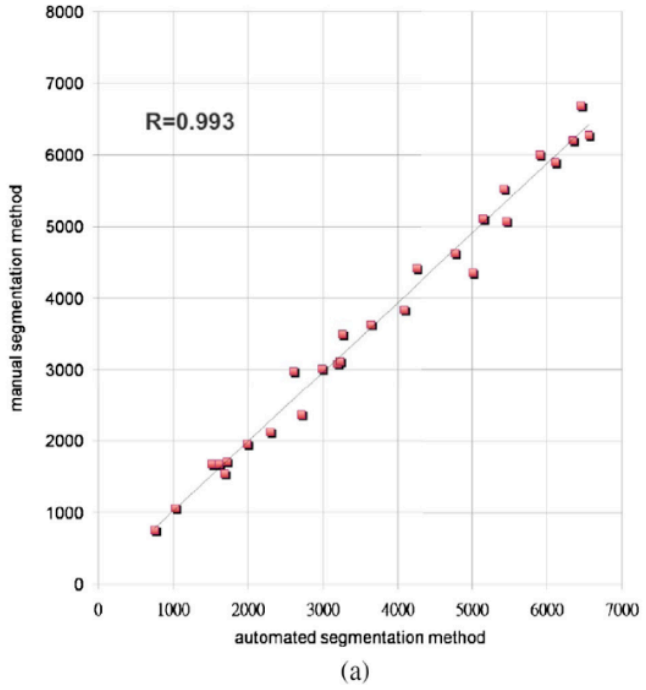

(a)

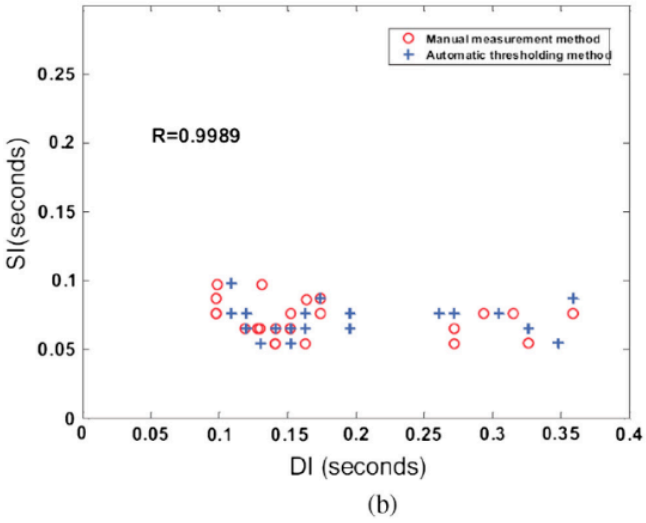

(b)

Fig. 5 (a) Correlation of the segmentation results of area μm^2 between the automated and manual methods. (b) Canonical correlation results of DI and SI using the automated thresholding and manual methods. R, correlation coefficient.

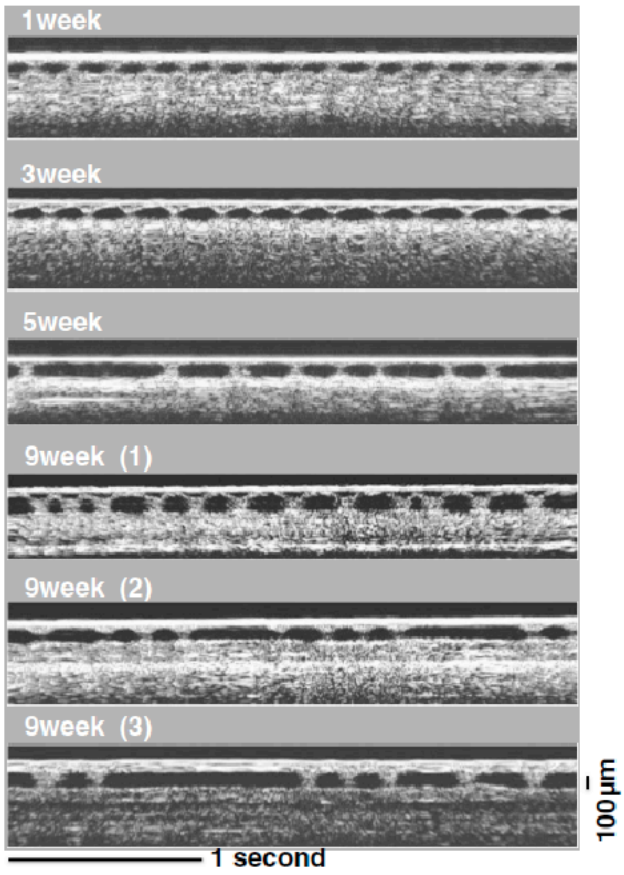

Fig.6 A representative M-mode OCT images in male *Drosophila* $\mathbf{w}^{1118}$ at one, three, five, and nine weeks of age.

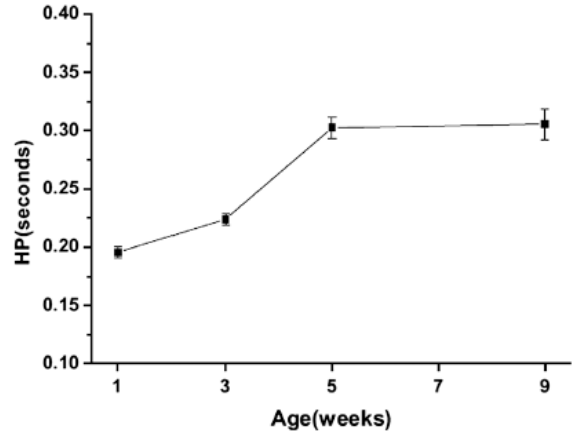

(a)

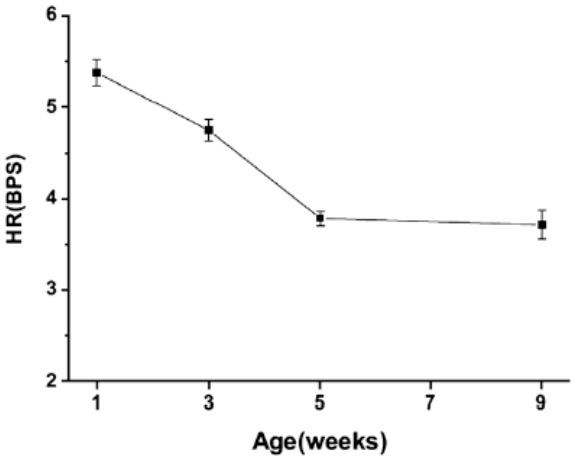

(b)

Fig.7 Cardiac parameters in male *Drosophila* $\mathbf{w}^{1118}$ at one, three, five, and nine weeks of age showing (a) HP and (b) HR.

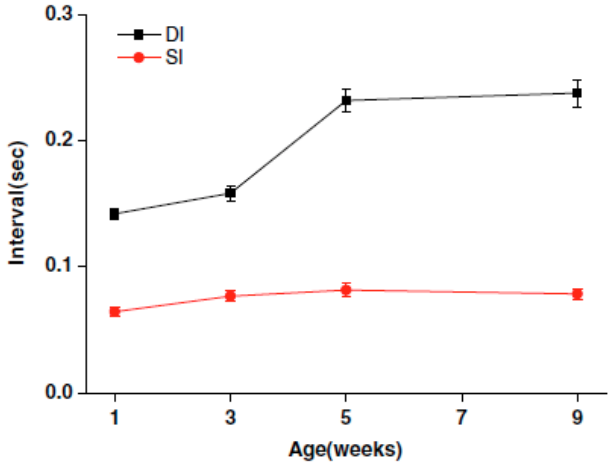

Fig.8 Cardiac parameters in male *Drosophila* $\mathbf{w}^{1118}$ at one, three, five, and nine weeks of age showing DI and SI.

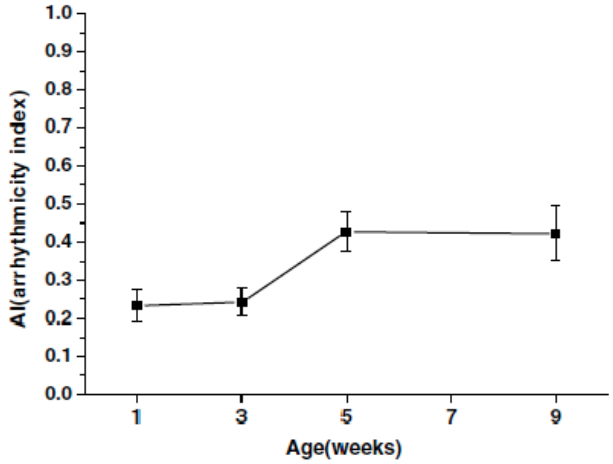

Fig.9 Cardiac parameters in male *Drosophila* $\mathbf{w}^{1118}$ at one, three, five, and nine weeks of age showing AI.

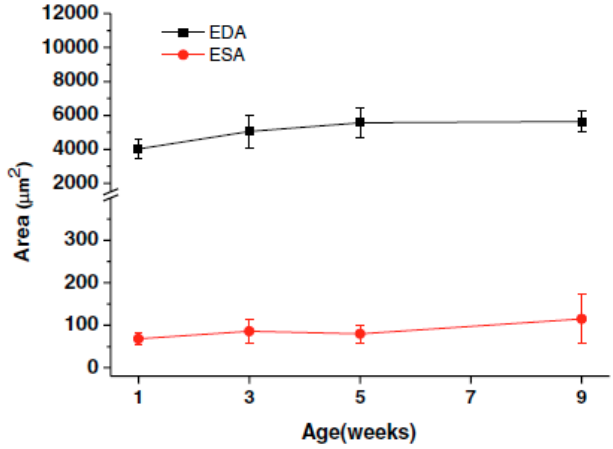

(a)

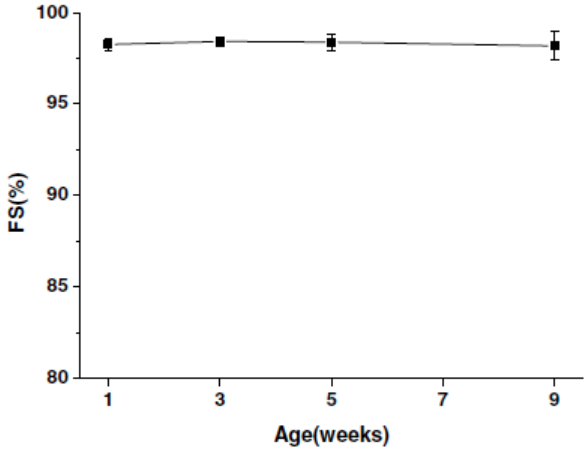

(b)

Fig.10 Cardiac parameters in male *Drosophila* $\mathbf{w}^{1118}$ at one, three, five, and nine weeks of age showing (a) EDA and ESA and (b) FS.

Chapter Ⅲ. Acer mutants impair contractile properties of Drosophila heart

1. Introduction

The Renin-angiotensin system (RAS) is an important regulator of blood pressure homeostasis, in which the protease renin cleaves the angiotensinogen into the angiotensin I (Ang I), followed by further cleaving of the Ang I by the angiotensin-converting enzyme (ACE) into angiotensin II (Ang II), thereby resulting in blood vessel contraction and hypertension (Santos, Krieger et al. 2012). With hypertensive cardiovascular disease the leading cause of death worldwide, pharmacological inhibition of the ACE and Ang II receptors has been demonstrated to be beneficial for ameliorating heart impairment (Volpe 2012) . The discovery of the ACE2, the Angiotensin- converting enzyme (ACE) homologue, has introduced further complexities into the canonical RAS signal cascade, as the major biologically active product of ACE2 will hydrolyze Ang II to form Ang 1-7, thereby counterbalancing the ACE activity (Donoghue, Hsieh et al. 2000, Tipnis, Hooper et al. 2000). It was thus believed that the primary function of the ACE2 is to regulate the blood pressure homeostasis (reviewed in (Keidar, Kaplan et al. 2007, Wang, Bodiga et al. 2012, Burrell, Harrap et al. 2013)).

Recent biochemical studies revealed that the ACE2 may modulate the RAS and thus impact the blood pressure regulation in vitro

(Donoghue, Hsieh et al. 2000). Several animal models have been used to explore the biological functions of the *ACE2* in vivo (Crackower, Sarao et al. 2002, Gurley, Allred et al. 2006), and genetic inactivation of the *ACE2* has been shown to impair the cardiac functions in mice (Crackower, Sarao et al. 2002, Gurley, Allred et al. 2006). Nevertheless, mutation of Angiotensin-converting enzyme-related (ACER), a *Drosophila* ACE2 homolog, was proven to result in a severe defect during heart morphogenesis (Crackower, Sarao et al. 2002). Other than its function in heart development, ACER also plays an important role in regulating sleeping behavior as flies lacking ACER generally experience reduced night-time sleep and exhibit greater sleep fragmentation (Carhan, Tang et al. 2011).

As outlined above, the mammalian ACE2 regulates mainly cardiac contractility, whereas *Drosophila* ACER regulates heart development during embryogenesis (Crackower, Sarao et al. 2002). Apart from than this distinction, ACER likely also regulates the heart physiology in adult flies as it is expressed in the heart of *Drosophila* during development (Houard, Williams et al. 1998). However, the issue of whether ACER regulates the physiological functions of adult flies has not been explored in depth. Here, we took advantage of a non-invasive Optical Coherence Tomography (OCT) imaging method to assess whether ACER modulates cardiac functions in living adult flies.

Optical coherence tomography (OCT), introduced in 1991, is a powerful tool for obtaining non-contact and non-invasive tomographic images of biological tissues (Huang, Swanson et al. 1991). In essence, OCT entails combining a broadband light source and a Michelson interferometer with a short coherence gate. The differences in the intensities of the backscattered light from the tissue are then analyzed to generate structural imaging. With the ability to image up to 3 mm in depth and achieve better than 15 micrometers in axial resolution, OCT fills the niche between ultrasound and confocal microscopies (Huang, Swanson et al. 1991). OCT had previously been successfully utilized to obtain in vivo images of the living heart in *Drosophila* (Choma, Izatt et al. 2006, Wolf, Amrein et al. 2006, Bradu, Ma et al. 2009, Choma, Suter et al. 2010, Ma, Bradu et al. 2010, Tsai, Chang et al. 2011, Guo, Liao et al. 2013). Moreover, combining the frequency domain OCT system with the recently developed frequency swept source OCT (SS-OCT) further improves the detection sensitivity, thereby rendering rapid B-Mode, M-mode, and Doppler OCT imaging of *Drosophila* possible (Bradu, Ma et al. 2009, Choma, Suter et al. 2010, Ma, Bradu et al. 2010, Tsai, Chang et al. 2011, Guo, Liao et al. 2013).

In this study, we applied SS-OCT and a novel algorithm (Guo, Liao et al. 2013) to evaluate the cardiac functions of *Drosophila*. Cardiac parameters, including the heart rate (HR), end-diastolic diameter (EDD), end-systolic diameter (ESD), and percent fractional shortening (%FS),

were automatically calculated from a large numbers of heartbeat M-mode OCT records. We found that the aforementioned contractile parameters declined with age in wild-type *Drosophila*. The age-dependent physiological functions of the heart were significantly reduced in *Acer* knock-down flies. Additionally, down-regulation of *Acer* increased the stress-induced heart failure rates and decreased the lifespans in flies, suggesting that ACER is both essential for the heart physiology and longevity of *Drosophila*.

2. Material and Methods

2.1 *Fly stocks and genetics*

We used $\boldsymbol{w}^{1118}$ flies as a wild-type control, and gal4 lines mesodermal and cardiac specific twist-24B gal4 and 24B-gal4 were obtained from the Bloomington Stock Center (Bloomington, IN). *Acer* mutant strains $Acer^{\Delta 164}$ and $Acer^{\Delta 168}$ were gifts from Alan D. Shirras (Carhan, Tang et al. 2011). *Acer* null lines were gained from CB-0338-3 flies via imprecise excision of the P {RS3} CB-0338-3 P-element, which is located in a region upstream of *Acer*. A pair of primers—*Acer* 1-5′ and Acer 1-3′—to include the first and second exon was used to acquire wild-type flies with a 1,400-bp amplification product. The checking of the *Acer* null mutants gave an approximately 1,100-bp polymerase chain reaction (PCR) product (Fig. 1) and confirmed the deletion sequences (Supplementary

Data Fig. 1a, 1b). All fly stocks and genetic crosses were maintained on standard yeast-glucose medium at 25°C.

2.1 Generation of transgenic flies

Two *twi*-24B-gal4 lines, a mesoderm and a heart driver (Lockwood and Bodmer 2002), were obtained from the Bloomington Stock Center.

To generate the *Acer* RNA interference construct, UAS- *Acer*-RNAi and *Acer*-cDNA (LD28328) were obtained from J. L Juang of the National Health Research Institutes of Taiwan. A 523 bp DNA fragment was PCR-amplified using a pair of primers, 5'-CGCGTCTAGAGTGCTGGAGGCGCGTAGGTTC-3' and 5'-CGCGTCTAGAGTCGGCATAGGAGCGGTGACC-3' (with the XbaI site underlined). The amplified DNA fragment was digested with XbaI and then cloned first onto the AvrII site. Subsequently the same DNA fragment was subcloned onto the NheI site of a pWIZ vector as described in (Lee and Carthew 2003). The orientation of the DNA construct was confirmed by restriction enzyme digestion. To generate transgenic flies, the standard germ-line transformation procedure using $\mathbf{w}^{1118}$ as the parental line was performed.

2.2 RT-PCR

RT-PCR was used to determine the silencing efficiency of the transgenic flies carrying the UAS-*Acer* RNAi construct. 3 flies carrying transgene

and $\mathbf{w}^{1118}$ driven by twi-24B gal4. PCR was performed using the *Acer*-specific primers *Acer* 2-1-3' CACAAACGGCTTCTCCGGAT and *Acer* 2-5' AACTGGCTTGGTATTG, as well as rps 17 primers 5'-CGAACCAAGACGGTGAAGAAG-3' and 5'-CCATAGAGGTAGTTCAACGTCC-3' assess the expression of the transgene. Phenotypic analysis of all the transgenic lines exhibited similar cardiac phenotypes. Several transgenic lines were obtained for *Acer*- Ri9, which exhibited the strongest silencing efficiency and was thus used for phenotypic analysis (Fig. 2 a, b).

2.3 SS-OCT measurements and automatic quantification of heart-beat parameters

To acquire the contractile parameters of adult flies, similar protocols were adopted (Wolf, Amrein et al. 2006, Guo, Liao et al. 2013). Briefly, in each experiment, two-dimensional (2-D) OCT images were first obtained in the longitudinal direction to identify the dorsal midline of the A1-A3 abdominal segments of the *Drosophila*. Then, the OCT image orientation was rotated by 90°, such that the conical chamber (CC) of the heart was acquired in the transverse plane. Measurements were always made in the same location in abdominal segment. A group of 20 flies were examined with a SS-OCT system (OCM1300SS, Thorlabs Inc., Newton, New Jersey). The median wavelength of the SS-OCT system was 1310 nm, with an axial resolution of ~12 μm in tissue, a total power of 10 mW, and

an A-scan rate of 16 kHz. Since heart function of *Drosophila* is decelerated greatly between 5 to 7 weeks of age, to assess the age dependent heart-beat parameters 1-week-, 3-week-, and 7-week-old flies were used. It has been previously reported that anesthetic treatment induces cardiac arrhythmias in mice, and that carbon dioxide or ether affects heart performances in *Drosophila* (Paternostro, Vignola et al. 2001, Roth, Swaney et al. 2002, Wessells and Bodmer 2004). To sidestep the aforementioned issues, during the image assessment, the *Drosophila* were first anesthetized with tri-ethyl amine and gently immobilized on wax gel with the dorsal side facing the OCT probe. The flies were subsequently allowed to return to a fully awake state on the bench for 20 minutes before being subjected to OCT scanning.

Fig. 3 is a representative video depicting a transverse 2-D OCT image of the conical chamber (CC) in the heart during diastole and systole in 1-week-old wild-type *Drosophila*. By acquiring in-depth scans at the midline of the CC over time without scanning, one can obtain an M-mode image of the vertical movements of the edges of the heart (y-axis) over time (x-axis). M-mode OCT images can provide the contraction pattern which give us an objective assessment of heart wall motion.

We then employed a semiautomatic algorithm we had previously proposed (Guo, Liao et al. 2013) for rapid analysis of the beat-to-beat contraction-relaxation parameters of the heart in *Drosophila* by using semi-automatic cardiac chamber segmentation in B-mode OCT images based on the random walker algorithm. Random walker (Grady L, 2004) is a semi-automatic segmentation method based on graph theory that can provide a unique solution that is robust to weak/noisy object boundaries, such as the cardiac tube of *Drosophila*. Further details and proofs can be found in Reference (Grady 2006). Briefly, after contrast-enhancement of the image, we created an initial set of seed points on the first frame. In the next frame, the cross-sections of the heart tube are automatically segmented in a total of 2000 frames, and the size of the inner margin is represented by area for each Drosophila. Then, depending on the histogram distribution of the changing area during each heart beat cycle, various contractile parameters, including the heart rate (HR), end-diastolic diameter (EDD), end-systolic diameter (ESD), and fractional shortening (%FS) were determined accordingly (see Ref. (Guo, Liao et al. 2013) for details). The FS was calculated as $[(EDD - ESD)/EDD] \times 100$, which represents the extent of the changes in the cardiac diameter during systole; it can provide an estimate of the contractility of the heart tube.

2.4 Electrical pacing

To monitor the stress-induced cardiac performance of adult flies, external heart pacing stress protocol was adopted and modified (Choma, Izatt et al. 2006). For each genotype, 100 flies were anesthetized with FlyNap® (Carolina Biological Supply Company, Burlington, NC) for 3 minutes and 30 seconds, and paced with a standard square wave stimulator at 40 V and 6 Hz for 30 s. By heart failure, we meant that either cardiac arrest or fibrillation was observed via the phase difference microscope within 2 minutes. The failure rate is defined as the number of flies with heart failure divided by the total number of flies.

2.5 Survivorship assay

A group of 10 newly enclosed flies were collected and cultured with standard media in a vial at 25 ℃. Viable flies were scored and transferred to a new vial every 5 days. The log-rank test (Peto and Peto, 1972) was performed to determine the differences in the lifespan of the flies.

2.6 Statistical analyses

Statistical analyses were performed using SPSS (version 14.0, SPSS Inc.). *P* values < 0.05 were considered to be statistically significant. The relative differences between two groups were compared using the Student's t test; ***, $p<0.001$; **, $p<0.01$; *, $p<0.05$.

3. Results

3.1 Acer mutants impair contractile properties of Drosophila heart.

Previous studies have indicated that ACER is critical for heart morphogenesis in *Drosophila* (Crackower M. A. 2002). Nevertheless, the function of ACER in heart physiology has not been precisely determined. To address this question of function, we used LOF flies (RNA interference to knock down *Acer* expression; *Acer* null mutants) and GOF lines (*Acer* overexpression flies) to increase *Acer* expression related to that in *Acer* null flies. The expression of the silencing construct was driven by a mesodermal- and cardiac-specific *gal4* driver, *twi-24B gal4*, using a UAS/gal4 system (Brand and Perrimon 1993). Quantitative RT-PCR showed that the knock-down efficiency of a double-stranded *Acer* RNA interference construct in late fly embryos was moderate. In comparison to expression in the control *twi-24B gal4* flies, the relative expression level of *Acer* mRNA was 45% in *Acer* knock-down flies *twi-24B gal4>* UAS *Acer Ri9*. The absence of 380 bp *Acer* mRNA in the $Acer^{\Delta 168}$ and $Acer^{\Delta 164}$ lines demonstrated that they were *Acer* null lines (Fig. 2 a, b). Carhan and others have generated null mutants ($Acer^{\Delta 168}$, $Acer^{\Delta 164}$) from imprecise excision of the RS P-element in CB-0338-3 flies, in which an RS3 element is inserted within the start codon of the *Acer* gene at the 2L: 8521983 position. When the null mutants were sequenced both forward and backward, the $Acer^{\Delta 168}$ line showed a deletion of 329 bp; the $Acer^{\Delta 164}$ line showed a deletion of 331 bp,

including most of the 5′ untranslated region and the first 12 codons (Supplementary Data Figs. 1a, 1b).

Having successfully knocked down the expression of *Acer*, we next used SS-OCT imaging to acquire various heartbeat parameters. As shown in Fig. 3, a transverse image of the conical cardiac chamber (CC) of an adult *Drosophila* underneath the dorsal midline of the A1–A3 abdominal segments was obtained using SS-OCT. The cardiac chamber contracted rhythmically with occasional irregular pulsing activities. Because the flies lack red blood cells in their circulatory fluids, the heart chambers appear as darker pixels on OCT. During heart contractions, the darker pixels corresponding to the edges of the heart tube crossed over to become lighter background pixels.

I found that *Acer* knock-down flies exhibited significantly enlarged systolic chamber dimensions with markedly impaired systolic functions, as demonstrated in the B-mode images (see Fig4). The representative M-mode OCT images of both wild type control and *Acer* knock-down flies at 1, 3, and 7 weeks of age are also shown in Fig. 5. The results for *Acer* knock-down *Drosophila* at various ages conclusively indicated impaired systolic functions with enlarged diastolic and systolic diameters compared with results for wild-type flies.

To assess more thoroughly the age-dependent contractile properties of *Drosophila*, we computed parameters including HR, end-diastolic diameter (EDD), end-systolic dimension (ESD), and FS from wild-type

and *Acer Ri* flies at various ages. Both wild-type and *Acer Ri* flies exhibited age-dependent declines in HR (Fig. 6a). Nevertheless, the HR of *Acer Ri* flies was consistently slower than that of wild-type flies, and the differences in average HR between wild-type and *Acer Ri* flies was more evident in aged animals (Fig. 6a). In young wild-type flies, the ESD was not significantly altered; however, it decreased in 7-week-old wild-type flies (Fig. 6b). Unlike ESD in wild-type flies, that in *Acer* knock-down flies increased with age (Fig. 6b). The EDD of wild-type flies was indistinguishable from that of the *Acer Ri* flies (Fig. 6c). However, the EDD of both wild-type and *Acer Ri9* flies decreased at the age of 7 weeks, and the EDD of *Acer Ri* flies was significantly larger than that of wild-type flies (Fig. 6c). Moreover, we found that the FS of wild-type flies did not decline with age (Fig. 6d). By contrast, that of *Acer Ri* flies declined consistently with age and was significantly decreased compared to that of wild-type flies (Fig. 6d). Because FS represents the extent of change in the cardiac chamber during systole and can be used as an index of cardiac contractibility, our results suggested that the down-regulation of *Acer* impaired the contractile properties of the *Drosophila* heart.

I observed the cardiac parameters of *Acer* null mutant flies with absent mRNA and protein (Carhan, Tang et al. 2011) using OCT measurement. HR, HP, and diastolic interval of $Acer^{\Delta 164}$ mutants increased similarly at 1 week and 3 weeks, whereas those of $\boldsymbol{w}^{1118}$

increased particularly at 3 weeks but not at 5 weeks (Figs. 7, 8). Surprisingly, we also discovered significant abnormalities in the EDA) ($p < 0.01$ and ESA ($p < 0.01$) of $Acer^{\Delta 164}$ mutants (Fig. 10). Thus, *Acer* mutant homozygotes in every age group had both cardiac systolic dysfunction and dilation causing cardiac chamber enlargement, as well as severe impairment in FS (Fig. 12). Of particular interest, the arrhythmicity index (AI) of $Acer^{\Delta 164}$ lines are higher than those of $\boldsymbol{w}^{1118}$, and arrhythmia was also produced earlier, at 3 weeks ($p < 0.01$; Fig. 11). Consequently, our cardiac parameters for *Acer* mutant flies were in accordance with those of Crackower (Crackower, Sarao et al. 2002) and others who have reported insufficiency of cardiac contractility in *ACE2*-disrupted mice. ACE2 is a protector in the control of the cardiovascular circulatory system and balances the level of ACE converted to AngII.

Ectopic *Acer* expression disrupts heart development as well as cardiac functions. Over-specification of cardial cells and misplaced cardial cells were observed when *Acer* was ectopically expressed by *twi*-24B gal4 and En-gal4 (Lin, 2004). WT embryo displayed normal cardiac phenotype. In my study, *Acer* overexpression flies displayed reduced cardiac contractility at 1, 3, and 5 weeks age and also exhibited cardiac asystole in ESD and FS (Fig. 13a, 13b). In particular, flies with increased ACER levels displayed a significant phenotype in percentage of FS starting at eclosion ($p < 0.01$). Donoghue (Donoghue, Wakimoto et al.

2003, Clark, Eisen et al. 2007) and others (Donoghue, Wakimoto et al. 2003, Clark, Eisen et al. 2007) have raised the issue of increased cardiac *ACE2* expression in transgenic mice being correlated with the incidence of sudden death and being conducive to severe, progressive conduction and rhythm disturbances.

I tried to rescue *Acer* null mutants with manipulation of 24B-gal4 to drive UAS-*Acer* expression. Surprisingly, the cardiac phenotype of *Acer* null mutants was altered toward normal even more than that of the control (Figs. 14–19). Although the standard error of the mean showed variation with age, that was a growing trend. The rescue effected significant results in UAS-*Acer* for *Acer* null mutants with respect to HP, DI, SI, EDA, ESA, AI, and FS. Gene therapy recovered heart function in *Drosophila*, greatly reducing cardiac dilation and contraction with respect to ESA and FS. AI of the rescued *Acer* null mutant was delayed at 3 weeks of age ($p < 0.01$).

This study examined EDA, ESA, AI, and FS through application and algorithms of the OCT technique. These parameters of cardiac function were superior for the assessment of impaired cardiac dilation, contraction, and arrhythmia.

3.2 ACER on cardiac performance of adult flies

As shown above, silencing the expression of *Acer* reduced the contractile properties of the *Drosophila* heart (Fig. 6), and the deficit in *Acer* is

likely also to affect the heart performance of flies. To test this possibility, we used a stress protocol to test stress-induced heart functions of *Acer* knock-down flies. We found that the down-regulation of *Acer* expression increased the likelihood of heart failure during electrical cardiac pacing in twi-24B gal4 crossed with *Acer* knock-down flies compared with controls at the ages of 1 week (heart failure rate 0.51 (23/45) versus. 0.36 (27/76), 2×2 χ^2 test, $p < 0.05$) (Ocorr, Akasaka et al. 2007) and 7 weeks (heart failure rate 0.76 (95/125) versus 0.57 (93/162), 2×2 χ^2 test, $p < 0.01$; Fig. 20). Because down-regulation of *Acer* affected both the contractibility and performance of the adult heart in *Drosophila*, we conclude that *Acer* is essential for the cardiac functions of *Drosophila* (see Fig. 6, 20).

We also found that *Acer* null mutant flies showed an increased incidence of failure of the heart to undergo electric pacing stress with age compared with that in $\boldsymbol{w}^{1118}$ control flies. Values of 0.52 (51/98), 0.58 (67/116), and 0.30 (34/115) failure were measured in $Acer^{\Delta 164}$ versus $Acer^{\Delta 168}$ versus $\boldsymbol{w}^{1118}$ at 1 week of age. Values of 0.76 (39/51), 0.56 (38/68), and 0.40 (38/95) failure were measured in $Acer^{\Delta 164}$ versus $Acer^{\Delta 168}$ versus $\boldsymbol{w}^{1118}$ at 3 weeks of age. Values of 0.90 (35/39), 0.67 (29/43), and 0.50 (34/68) failure were measured in $Acer^{\Delta 164}$ versus $Acer^{\Delta 168}$ versus $\boldsymbol{w}^{1118}$ at 5 weeks of age (Fig. 21). $Acer^{\Delta 164}$ lines appeared obviously intolerant after electric pacing stress at 1, 3, and 5 weeks of age (2×2 χ^2 test, $p < 0.001$).

Electrical pacing-induced heart failure in GOF flies (twi-24B

gal4-driven UAS-*Acer*) increased 0.22%, 0.22% and 0.15% compared with the controls at 1, 3, and 5 weeks of age. The overexpression of *Acer* had no beneficial effects on fly hearts and produced no cardiac protective results (Fig. 22). We observed that overexpression of *Acer* completely rescued null mutant lines with respect to electrical pacing-induced heart failure. The heart failure rates of $Acer^{\Delta 164}$; UAS-*Acer* /24B versus $Acer^{\Delta 168}$; UAS-*Acer* /24B versus 24B gal4/+ were 0.33 (32/98), 0.33 (28/85), 0.37 (69/184) at 1 week of age; 0.40 (36/90), 0.41 (43/105), and 0.50 (73/144) at 3 weeks of age; and 0.51 (61/120), 0.48 (60/126), and 0.54 (105/194) at 5 weeks of age. No differences occurred on 2×2 χ^2 test, $p > 0.05$ (Fig. 23).

3.3 Necessity of ACER for longevity in Drosophila

Modulation of the gene expression in the heart can alter the longevity of *Drosophila* (Wessells, Fitzgerald et al. 2004). As shown above, cardiac-specific down-regulation of *Acer* exacerbated the age-dependent cardiac functions of *Drosophila*. We posit that the down-regulation of *Acer* directly impacts the longevity of the flies as well. Survivorship assay showed that the mean lifespans of control *twi-24B gal4*, *twi-24B gal4> Acer Ri9*, and *twi-24B gal4>*UAS-*Acer* flies were 66.85, 54.90, and 57.3 days, respectively (Fig. 24). Statistical analyses revealed that the differences in survivorship of the wild-type control and *Acer* knock-down flies were significant (log rank test, $p < 0.001$), and overexpression of

Acer flies showed a similar effect of decreased survivorships. As a result, the *Acer* null mutants $Acer^{\Delta 164}$ and $Acer^{\Delta 168}$ had short longevity compared with that of $\boldsymbol{w}^{1118}$ (log rank test, $p < 0.001$; Fig. 25). The activity of *Acer* is essential for the survival of the flies; *Acer* knock-down, deletion mutant, and overexpression flies displayed decreased lifespans. 24B gal4-driven UAS-*Acer* rescued the survivorship of Acer null mutants (see Fig. 25). Lifespan curves of $Acer^{\Delta 164}$; UAS-Acer/24B and $Acer^{\Delta 168}$; UAS-Acer/24B and 24B gal4/+ approached considerably ($\chi^2 = 2.6$; 1.4, log rank test, $p = 0.107$; 0.238; Fig. 26). *Acer* influenced cardiac performance and then impacted life expectancy (Coldman and Elwood 1979).

4. Discussions and Conclusion

The present study is the first investigation of in vivo functional changes in the heart of *Acer* knock-down and mutant flies. It has been reported that the disruption of the ACER results in a severe and lethal defect during heart morphogenesis in *Drosophila* (Crackower, Sarao et al. 2002). Nevertheless, genetic analysis of the same *Acer* mutant allele revealed that there existed a second mutation on the secondary chromosome, in which case it was likely to contribute to the embryonic lethality of the *Acer* mutant allele (unpublished observation by M.T. Su). To sidestep this complicated issue and to better ascertain whether ACER plays a

physiological role in adult animals, we adopted the RNA interference approach. Our data indicated that *Acer* knock-down flies exhibited age-dependent changes in both the heart beating and the contractility of the heart tube. Compared with the wild type control, the cardiac performance and lifespan were reduced when *Acer* was down-regulated, suggesting that ACER is essential for both adult heart physiology and longevity of *Drosophila*.

Although we have shown that the HR of wild-type control flies is reduced in an age dependent manner (Fig. 6a), our results are less significant as compared with other studies (Wessells, Fitzgerald et al. 2004). Since heartbeat of *Drosophila* is both myogenic and neurogenic, it is affected by temperature, aging, genetic background as well as anesthetic agent (Wessells and Bodmer 2004, Fink, Callol-Massot et al. 2009). To reduce variability of heartbeat, decapitated flies were used as previously reported (Ocorr, Reeves et al. 2007, Fink, Callol-Massot et al. 2009). As we have used OCT to obtain the heartbeat parameters form live flies in this study, it is expected that variability of heartbeat is increased which may reduce the statistical significance. However, the differences in the HR between wild-type and *Acer* Ri9 flies were more evident than in aged animals. On the other hand, due to differences in size between flies, large variations existed in both EDD and ESD within the tested groups; however, use of %FS can eliminate the effect of body size.

Although we have shown that down-regulation and mutant of ACER

affects the age-dependent heart functions and longevity, the mechanism by which *Acer* deficiency leads to the above phenotypes is not clear. It has been reported that the expression levels of NADPH oxidase and reactive oxygen species (ROS) formation were significantly higher in *ACE2* KO mice (Xia, Suda et al. 2011, Pena Silva, Chu et al. 2012). Angiotensin Ⅱ-mediated activation of AT1 receptor *o*f *ACE2* $^{-/y}$ mice activates the cascades of downstream pathway by G-protein-coupled receptor (GPCR) triggered. The age-dependent cardiomyopathy induced in ACE2 null mice develops severity with increase mitogen-activated protein kinase (MAPK) activation, NADPH oxidative stress, neutrophil accumulation, inflammatory IL-1β, IL-6 and collagenase MCP-1, MMPs levels, and cardiac hypertrophy (Oudit, Kassiri et al. 2007). ACE2 deficiency advances Ang Ⅱ-mediated profillin-1 expression, NADPH oxidase activity, superoxide and peroxynitrite production, which related with increase activation of the Akt-ERK-eNOS signaling pathway. And then causes inflammation, fibrosis, proliferation on the ACE2/Ang-(1-7)/Mas axis to be blocked. When AT1 blockade suppresses aortic inflammation and peroxynitrite production (Jin, Song et al. 2012). Since oxidative stress are elevated in congestive heart failure (CHF) patients and correlate well with the development and progression of cardiovascular diseases (reviewed in (Whaley-Connell and Sowers 2012)), it will be interesting to study in the future whether ROS levels also increase in the heart of *Acer* knock-down and mutant flies.

The molecular mechanisms of *Acer* gene effects on heart of *Drosophila*, that is currently unknown. Further studies need to illustrate the pathway of the mechanism on the changes level of downstream signal through the manipulation of gene. We used the cardiac parameters ESA, EDA, FS, and AI, which present significantly in diastolic and systolic heart failure. The treatment of cardiovascular disease remains a popular subject. Overexpression of *Acer* restores cardiac function and improves longevity in *Acer* null mutants. Increasing *Acer* level through gene therapy displayed heart protective effects in heart failure in *Drosophila*.

5. Figures

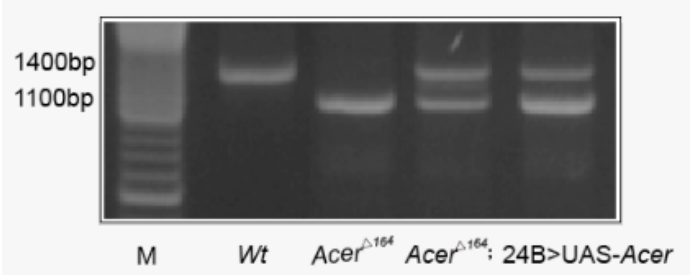

Fig. 1 Polymerase chain reaction (PCR) products exhibit the deletion of an approximate 1,100-bp *Acer* DNA fragment in the *Acer* null mutant $Acer^{\Delta 164}$, and mutant rescued flies exhibited both approximately 1,100 bp and 1,400 bp fragments with *Acer* 1-5′ and *Acer*1-3′ primer.

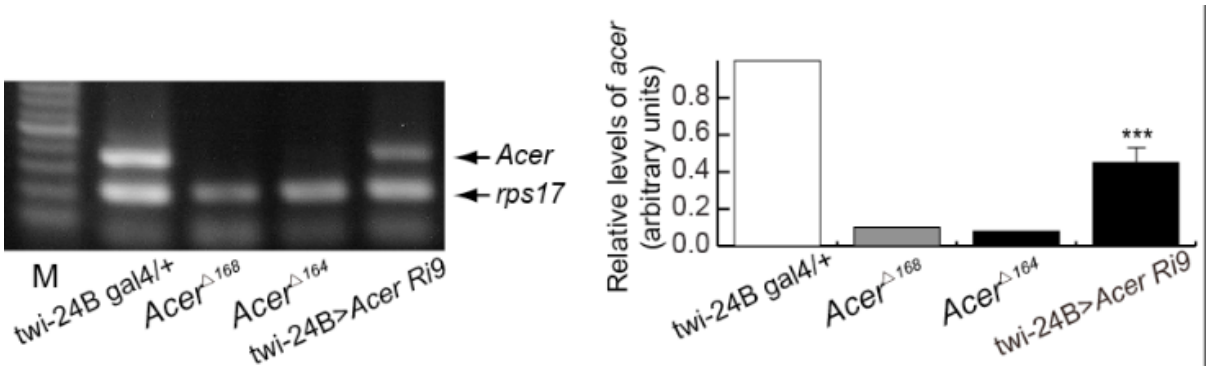

（a） （b）

Fig. 2 Expression levels of *Acer* messenger RNA (mRNA) in null lines and knock-down flies. (a) Complementary DNA PCR products of $Acer^{\Delta 168}$, $Acer^{\Delta 164}$, *twi*-24B>*Acer Ri9*. (b) Reverse transcription-PCR showed that the mRNA expression levels of $Acer^{\Delta 168M}$ and $Acer^{\Delta 164F}$ were null, and those of twi-24B>*Acer Ri9* were 45% of that in the wild-type control. Rps17 was used as loading control. The relative expression levels were compared using Student's *t*-test; ***, $p < 0.001$.

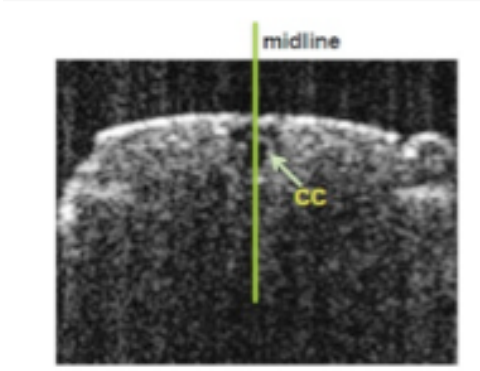

Fig. 3 A representative B-mode OCT in male *twi*-24B gal4/+ at 1 week of age.

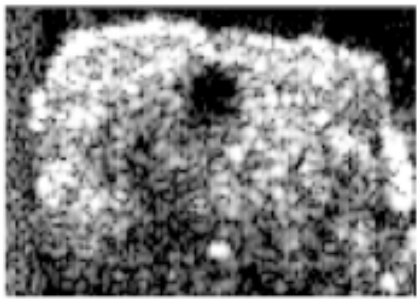

Fig. 4 A representative B-mode OCT image in *Acer* knock-down flies at 3 week of age.

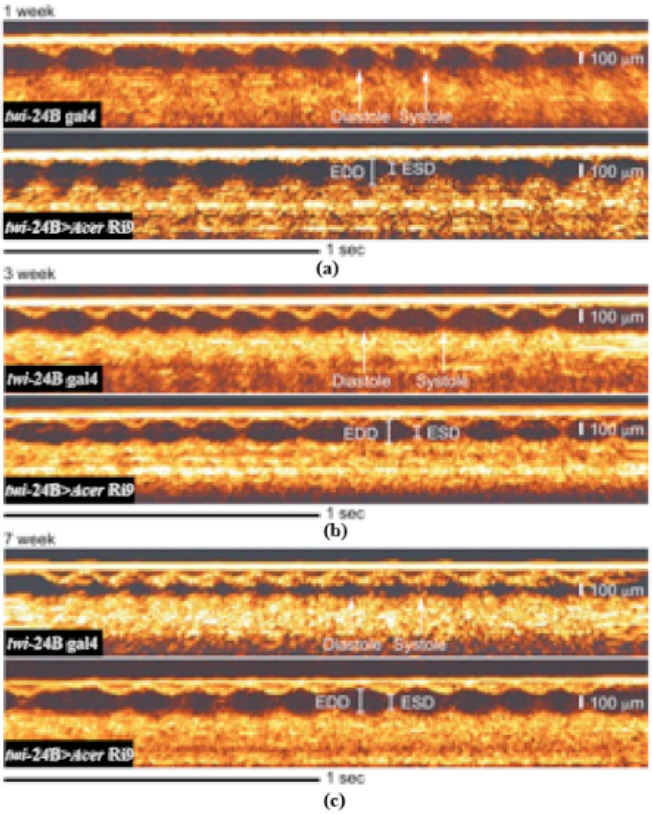

Fig. 5 Representative M-mode OCT images in wild-type control (*twi*-24B gal4/+) and *Acer* silencing lines (*twi*-24B > *Acer* Ri9) at one, three, and seven weeks of age.

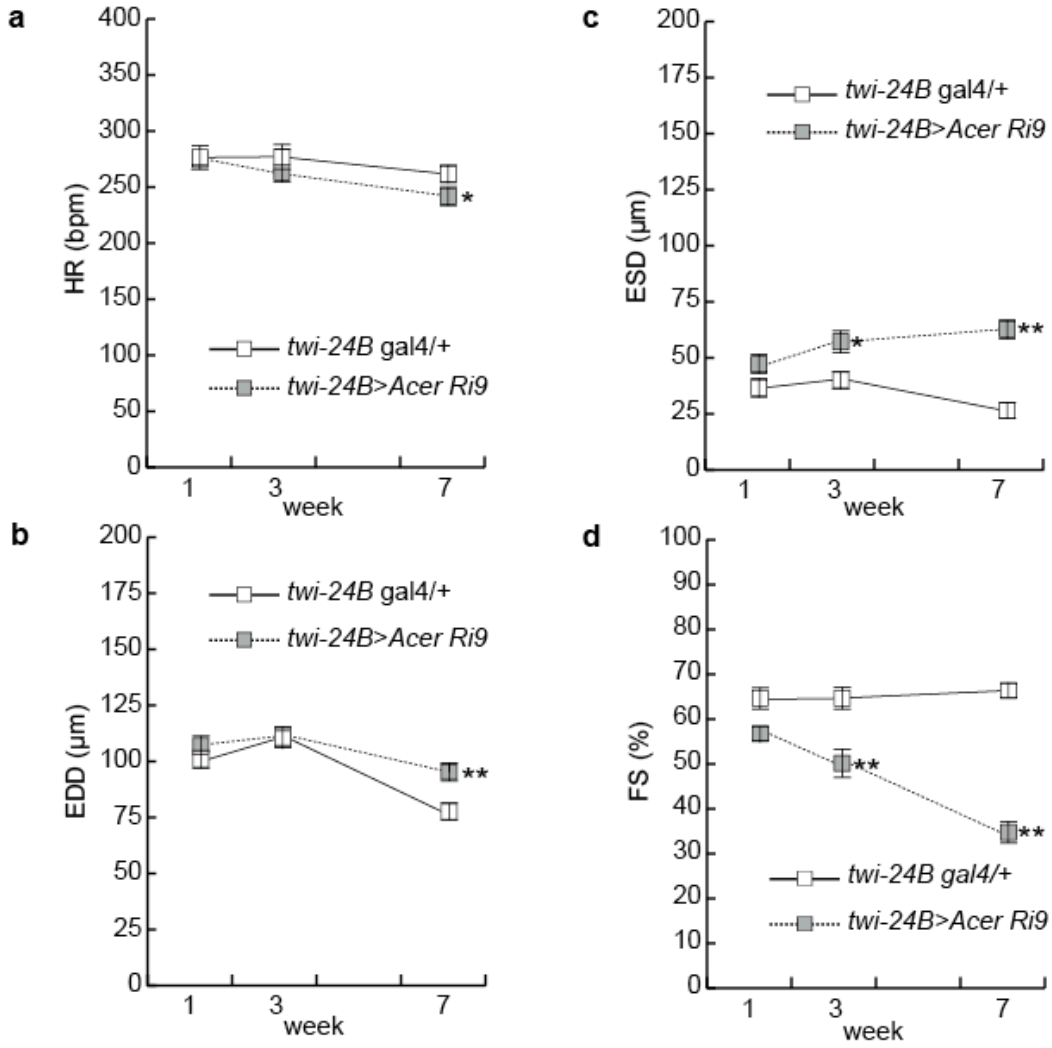

Fig. 6 Cardiac parameters in male wild-type control (*twi*-24B gal4/+) and *Acer* silencing lines (*twi*-24B > *Acer* Ri9) at one, three, and seven weeks of age showing (a) HR, (b) ESD, (c) EDD, and (d) %FS. Data points represent the mean (±SEM) for 20 flies per data point. *, $p < 0.05$; **, $p < 0.01$ by student's t test.

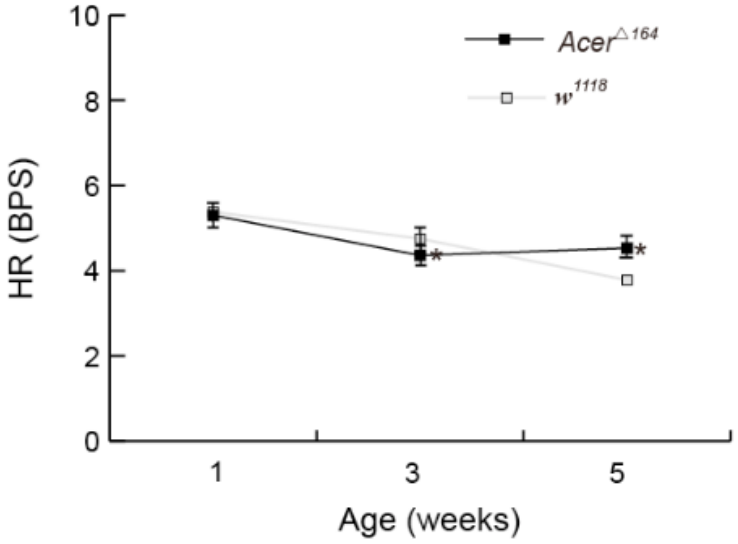

Fig. 7 Cardiac parameters in the *Acer* null mutant and $\mathbf{w}^{1118}$ at one, three, and five weeks of age showing HR. *, $p < 0.05$ by Student's t test.

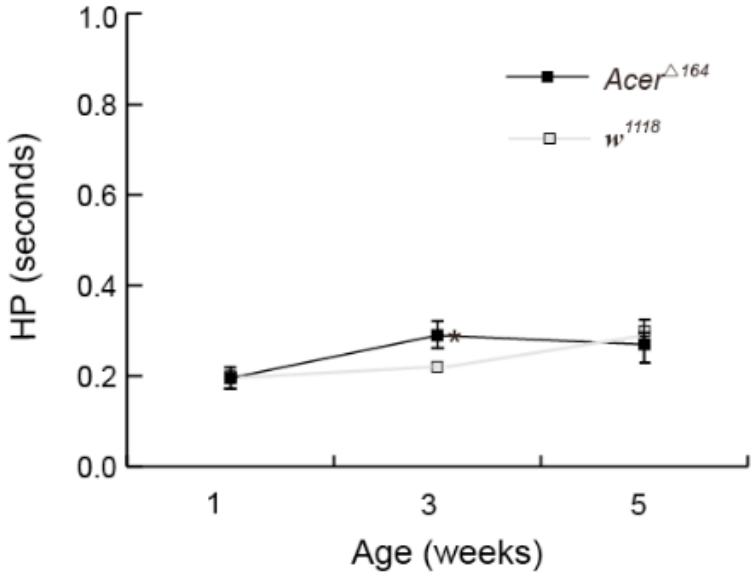

Fig. 8 Cardiac parameters in the *Acer* null mutant and $\mathbf{w}^{1118}$ at one, three, and five weeks of age showing HR. The *Acer* null mutant value was higher than that of $\mathbf{w}^{1118}$ at 3 weeks of age. *, $p < 0.05$ by Student's *t*-test.

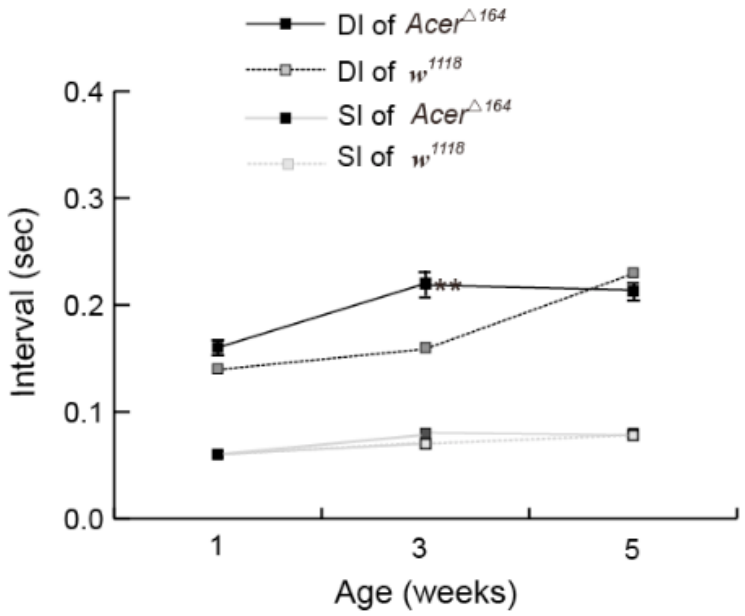

Fig. 9 Cardiac parameters in the *Acer* null mutant and $\mathbf{w}^{1118}$ at one, three, and five weeks of age showing DI and SI, which were similar except for DI at 3 weeks. **, $p < 0.01$ by Student's *t*-test.

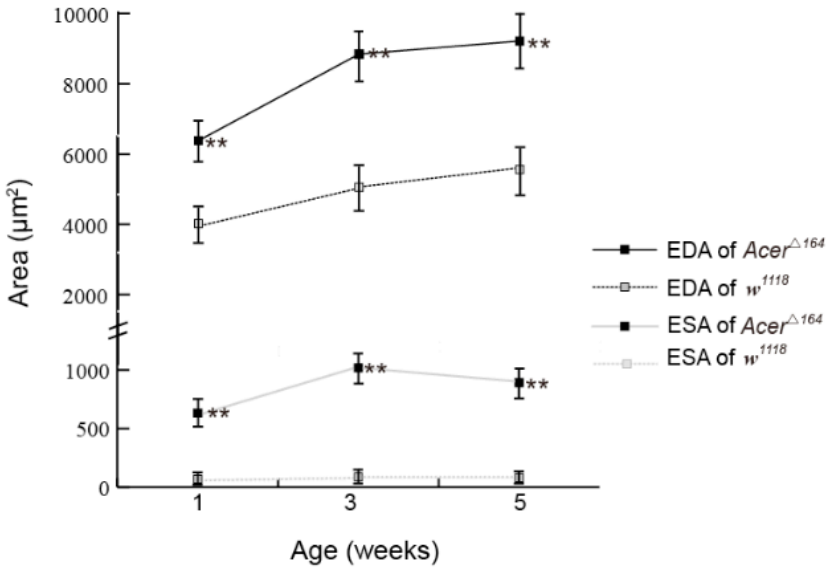

Fig. 10 Cardiac parameters in *Acer* null mutant and $\mathbf{w}^{1118}$ at one, three, and five weeks of age show EDA and ESA. The EDA and ESA values for the $Acer^{\triangle 164}$ mutant were significantly higher every week. **, $p < 0.01$ by Student's *t*-test.

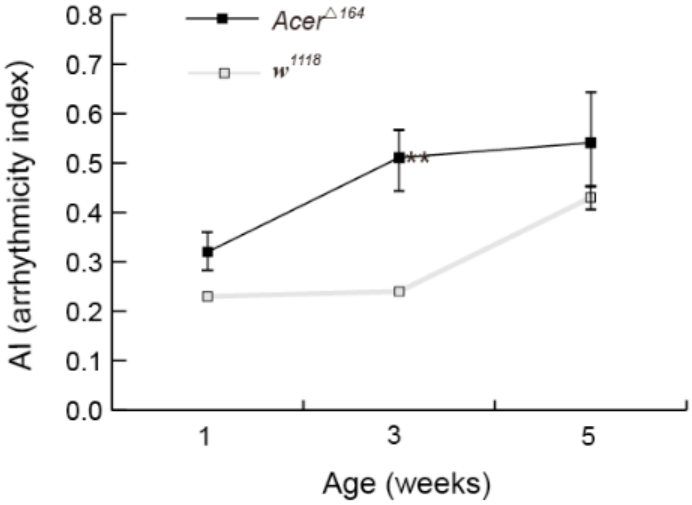

Fig. 11 The cardiac parameters of AI are higher in the *Acer* null mutant than in $\mathbf{w}^{1118}$ at one, three, and five weeks of age. Values in $\mathbf{w}^{1118}$ increase after the fifth week, but those in the $Acer^{\triangle 164}$ mutant increase early from the third week. **, $p < 0.01$ by Student's *t*-test.

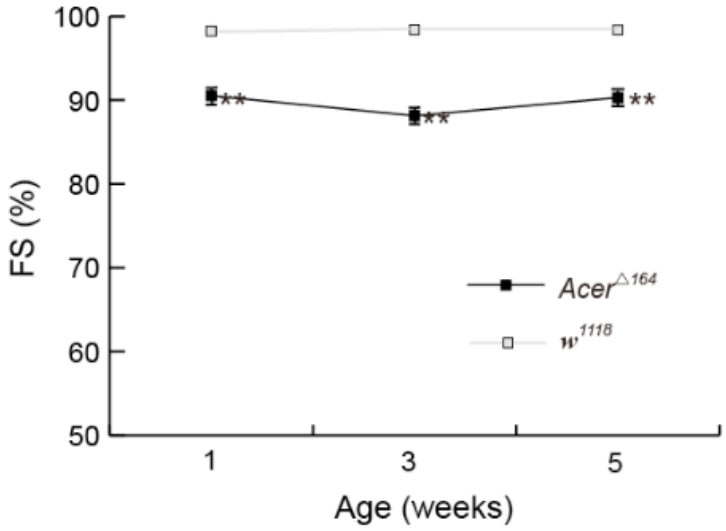

Fig. 12 *Acer* null mutant reduces cardiac parameter FS compared with that in $\mathbf{w}^{1118}$ at one, three, and five weeks of age. **, $p < 0.01$ by Student's *t*-test.

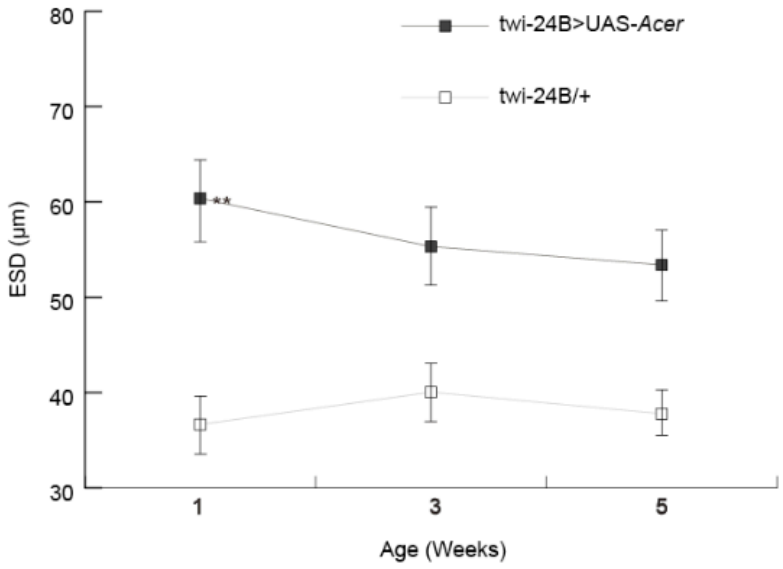

(a)

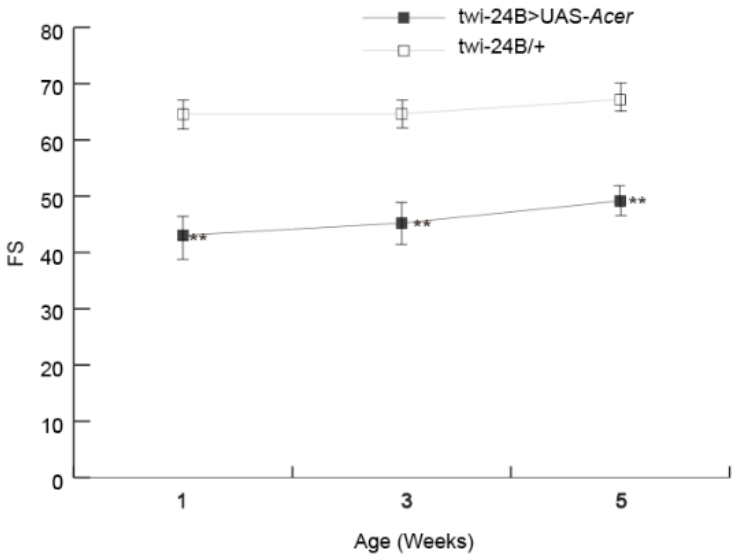

(b)

Fig. 13 *Acer* gain of funct ion flies with cardiac contractile dysfunction on OCT. (a) *Acer* overexpression flies at one, three, and five weeks of age showing ESD in micrometers and (b) FS (%). All data are expressed as means ± SEM for 20 flies per data point. **, $p < 0.01$ by Student's *t*-test.

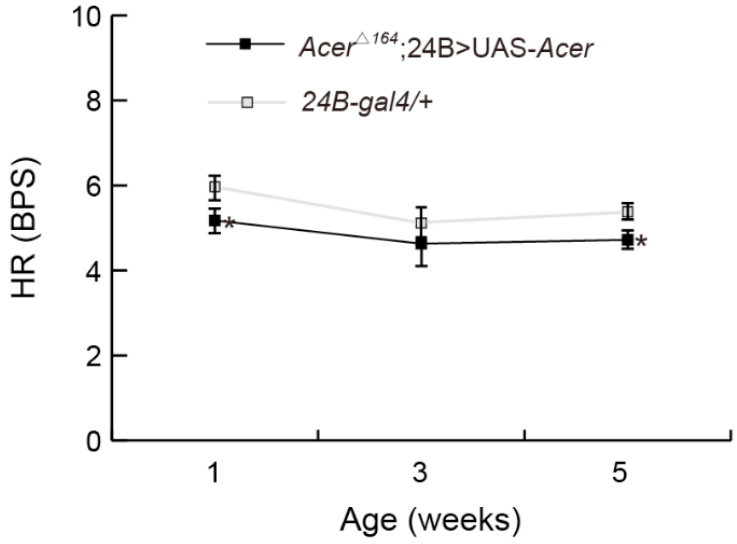

Fig. 14 Cardiac HR parameter of the *Acer* rescued lines was lower in and 24B-gal4 at one, three, and five weeks of age. *, $p < 0.05$ by Student's *t*-test.

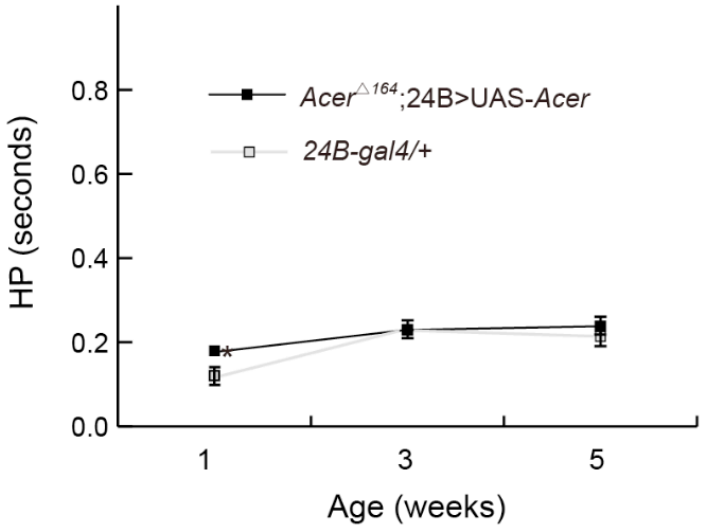

Fig. 15 Cardiac HP parameter was similar in the *Acer* rescued and 24B-gal4 lines at three, and five weeks of age. *, $p < 0.05$ by Student's *t*-test.

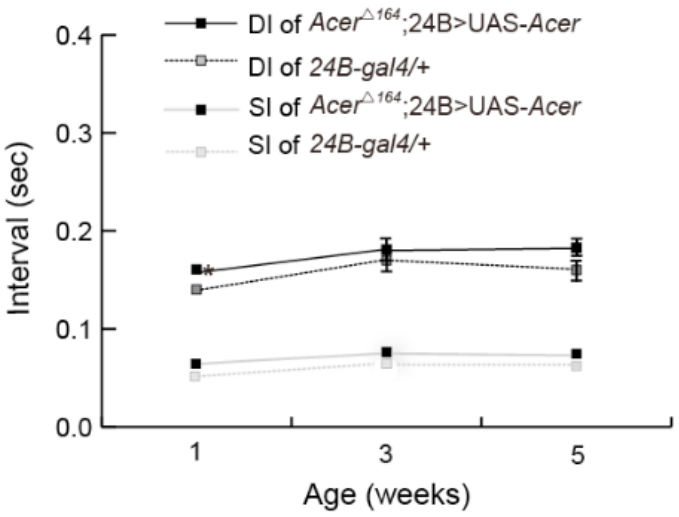

Fig. 16 *Acer* rescued line restored the interval between DI and SI in cardiac parameters compared with 24B-gal4 at one, three, and five weeks of age. *, $p < 0.05$ by Student's *t*-test.

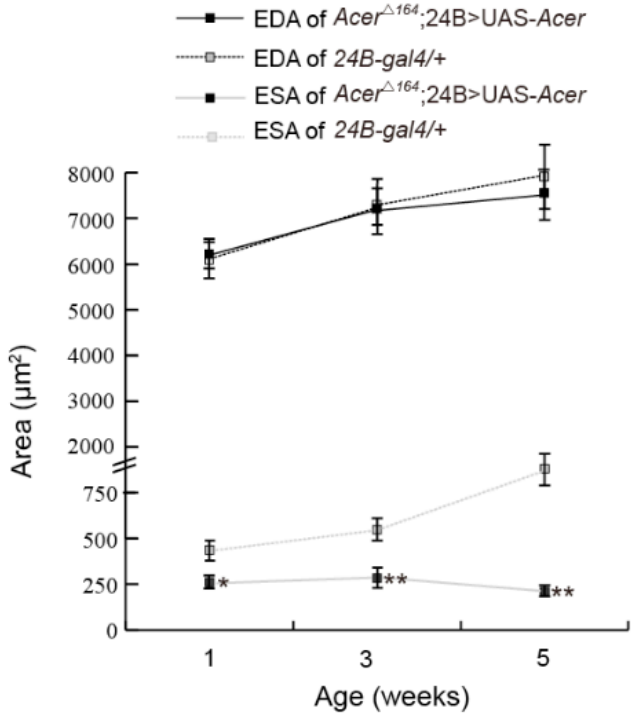

Fig. 17 *Acer* rescued line had EDA values comparable to those of 24B-gal4/+ at one, three, and five weeks of age, but the cardiac parameter ESA was higher in the *Acer* rescued line. *, $p < 0.05$; **, $p < 0.01$ by Student's *t*-test.

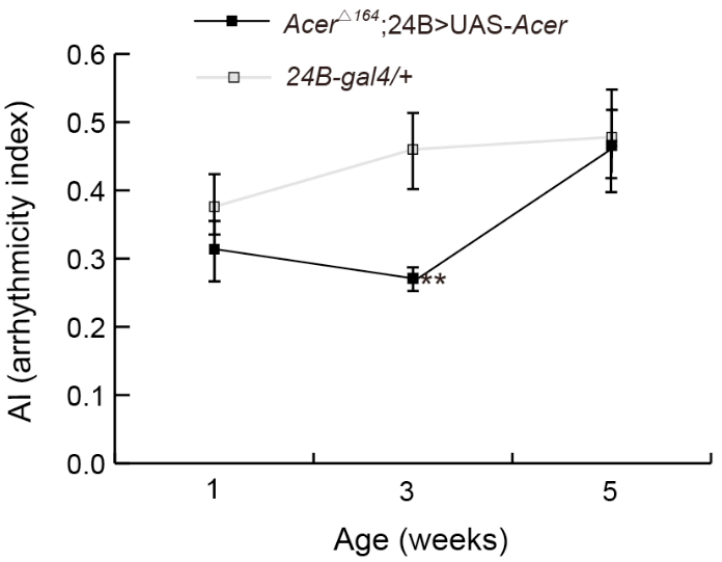

Fig. 18 Cardiac AI was similar in the *Acer* rescued and 24B-gal4 lines at one, three, and five weeks of age. $Acer^{\triangle 164}$ rescued line raises later on AI from the fifth week. **, $p < 0.01$ by Student's *s* test.

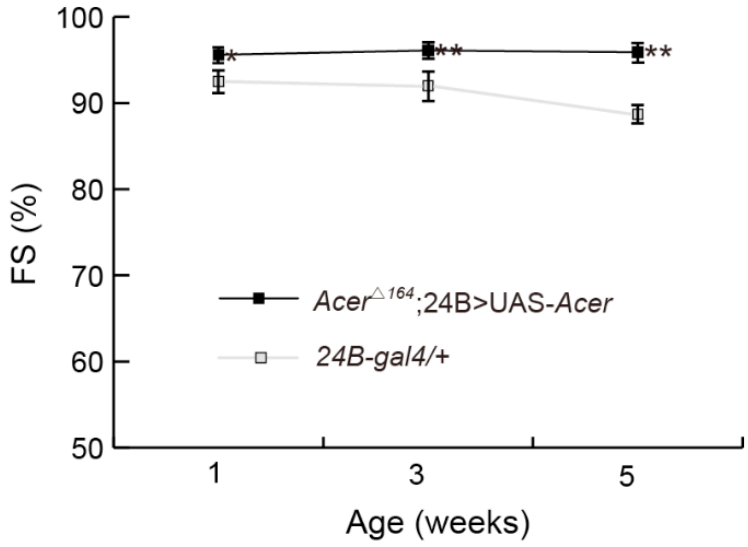

Fig. 19 Rescued *Acer* mutants restored FS cardiac function at ne, three, and five weeks of age. *, $p < 0.05$; **, $p < 0.01$ by Student's *t*-test.

.

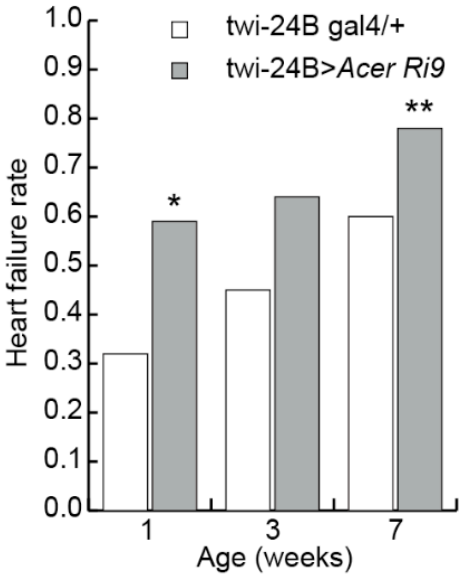

Fig. 20 Heart failure rate during electric pacing in both the wild type control (twi-24B gal4/+) and *Acer* silencing lines (twi-24B>*Acer Ri9*) at one, three, and seven weeks of age. *, $p < 0.05$; **, $p < 0.01$ by Student's *t*-test.

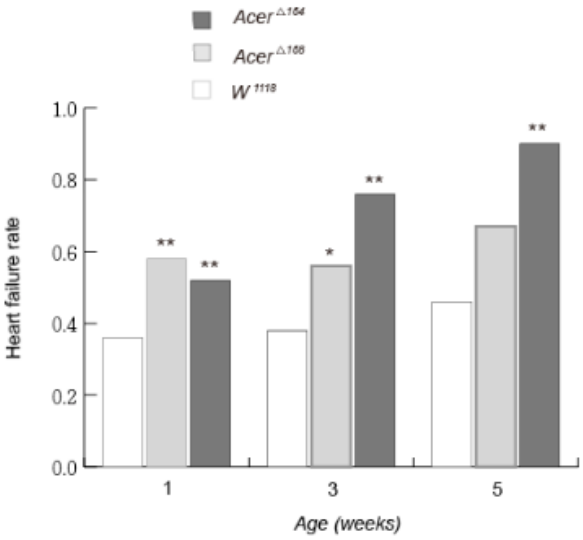

Fig. 21 Lack of *Acer* leads to heart failure compared to the wild-type condition. Statistically significance differences occurred in one, three, and five -week-old $Acer^{\triangle 168}$, $Acer^{\triangle 164}$, and wild type on electric pacing stress assay. *, $p < 0.05$; **, $p < 0.01$ by Student's *t*-test.

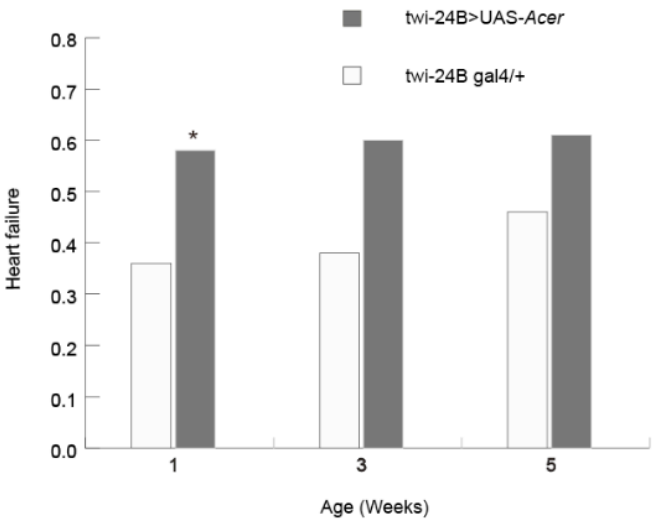

Fig. 22 Heart failure rate during pacing in both wild-type control (*twi*-24B gal4/+) and *Acer* overexpressed (*twi*-24B >UAS-*Acer*) at one, three, and five weeks of age. *, $p < 0.05$; **, $p < 0.01$*, by Student's *t*-test.

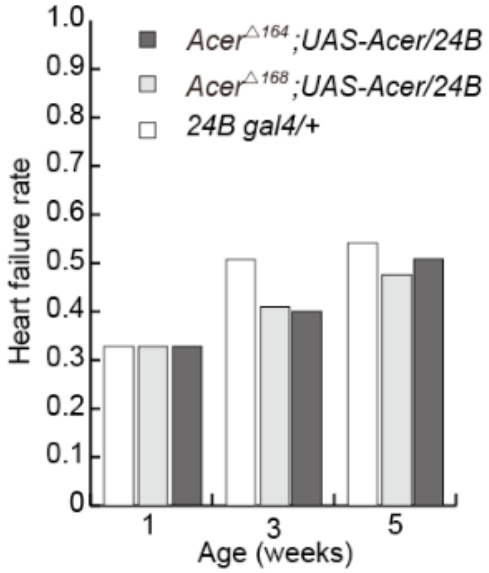

Fig. 23 Expression of *Acer* rescued the heart failure of *Acer* null mutants. One, three and five-week-old $Acer^{\Delta 168}$ and $Acer^{\Delta 164}$ were used for assay. The failure rates were not statistically significant between wild-type and rescued flies.

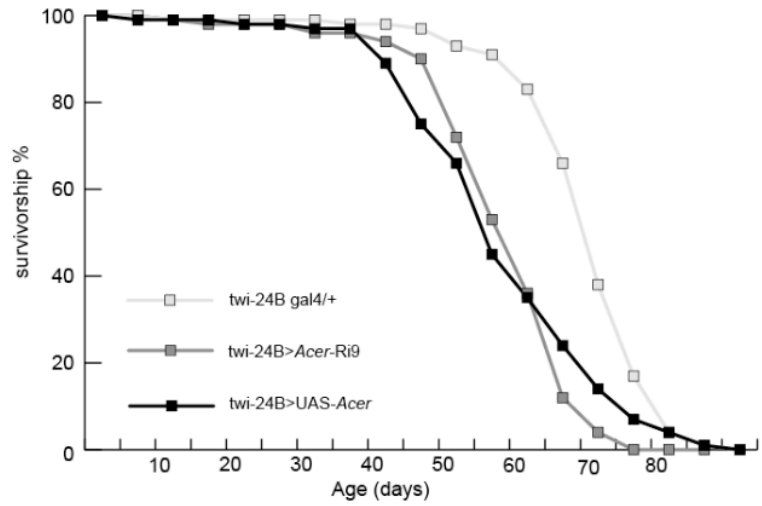

Fig. 24 Overexpression and down-regulation of *Acer* flies reduced the longevity of *Drosophila*. The survivorship curve displays wild type control (t*wi*-24B gal4/+), *Acer* silencing lines (*twi*-24B>*Acer* Ri9), and overexpressing lines (*twi*-24B>UAS-*Acer*) derived using log-rank analysis ($p < 0.001$).

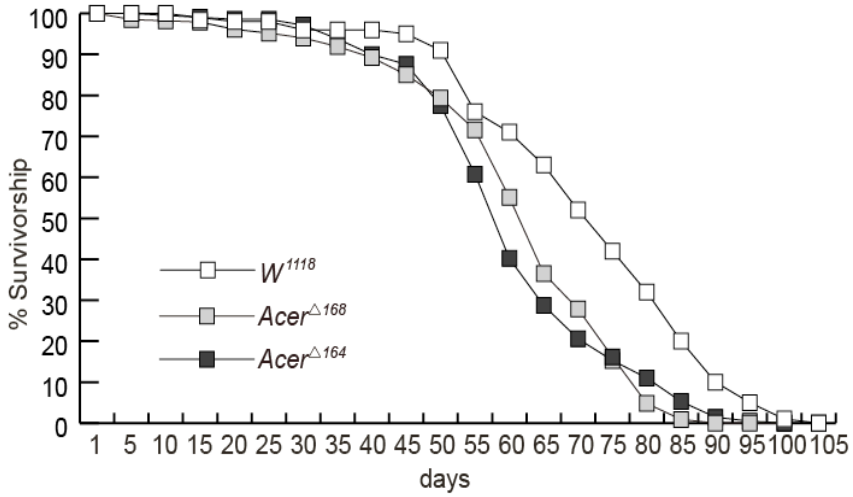

Fig. 25 Loss-of-function in the *Acer* null mutant reduced lifespan. $Acer^{\triangle 168}$ and $Acer^{\triangle 164}$ strains displayed decreased survivorship as analyzed by log rank test ($p < 0.001$).

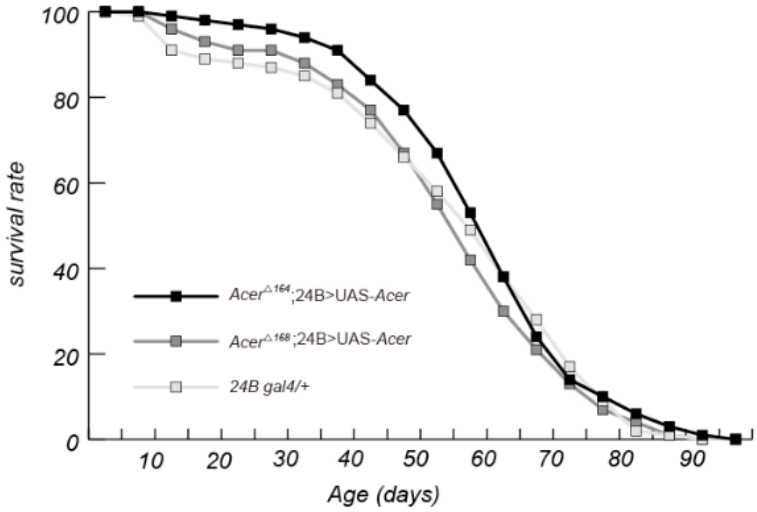

Fig. 26 Lifespan of *Acer* null mutants was restored by *Acer* expression. Survivorship assay was quantified using the log rank test (χ^2 of $Acer^{\triangle 164}$; UAS-Acer/24B, as well as $Acer^{\triangle 168}$; UAS-Acer/24B = 2.6; 1.4, log rank test, P = 0.107; 0.238).

Supplementary data

5’---CGACTTCTA
CCTTACCGTTTTTTATAATAATTAAAAAAATTCAATTTATTTCTAGTTTGTA
AAACAAAACTTTGAAAAATAAAATCCCGTTATTTTTACGAATACCCTACAC
GATTACGACTAACGCCTTTACAATACAATATCAGCTGACCACTTGAGTTT
GCTGTACAAAATACCGTTAGCGGTGCACTCAACAGCTGAGCGGCGCTCA
AGCTAACCCGCCGATAATGCAG
acaacaaaaaaagtattaagcaggtagattggcaggcaggtgtaaaatttcggaacacgcacactcttgt
gattgtgtatgaatgcgaaacggcgtacgctctcgcaaacgctcctacgagtataaaaaccgttctccgtcg
cagcaagcagtcagtatctccacagcagcagaggcgacgggaagacaaagcaatctgaattgaatacg
tcctagttttgggtccgtataacaaaaaaatttatagtgcaaagtagctgagataagcgcggcttgacccggg
aaaggcgccagagatgggggcatgcaatataacagtcttattgctggt
CATCATGTTGTGGGTGAGTTATATACGAACACAAGCCGCAAAGATTTCGA
TTATGTTCTATATTTAAACATTTGTATATATTTCATTAGCTACCCCATGGTC
TGTCCATGGGCAATAGCTGCTCGGCATCGGTGCTGGAGGCGCGTAGGT
TCTTCGAGCTGGAAAATGAACAATTGCGAAGGCGTTTCCATGAGGAATTC
CTTTCCGGCTACAACTATAACACCAATGTAACGGAGGCGAATCGCCAGG
CCATGATCGAAGTGTATGCCCGCAATGCGGAACTGAATAAGCGACTCGC
GCAGCAGATAAAGTCCTCCGATTACGTTCAGTCCGAGGATGCGGATATA
CGACGACAGGCCGAGCACCTATCCAAATTGGGTGCATCCGCTCTGAATG
CCGACGACTACCTGGCCCTGCAGAATGCCATCAGTTCGATGCAGACGAA
CTATGCTACCGCCACCGTGTGCTCGTACACCAATCGCAGTGATTGCTCT
CTCACCCTGGAGCCGCACATACAGGAGCGTCTGTCCCATAGCCGTGATC
CTGCCGAACTGGCTTGGTATTGGCGGGAGTGGCACGATAAGTCCGGAA
CTCCCATGCGGCAGAACTTCGCCGAGTATGTGCGACTGACGCGCAAGG
CATCTCAGTTGAATGGTAAGTGATGGACGCCTAGATAACCCCATGTCTGA
CCCAAATCGGGAGAAATCGGTTCGGGCCAGCACAGGGAGAATAGCTTAT
CCACTTGACATTTATCTGTGGTGAAGTACTTGGGTATTTATACCTAATCTC
GGTGTCA---3’

Fig. 1a *Acer*$^{\Delta 164}$ deleted a 331-bp DNA sequences with a forward primer, *Acer* 1-5′, and a reverse primer, *Acer* 1-3′; a 1,400-bp amplification polymerase chain reaction product was anticipated from the wild-type fly.

5’---GGGTCTTCT
CCTTAACCGTTTTTTATAATAATTAAAAAAATTCAATTTATTTCTAGTTTGT
AAAACAAAACTTTGAAGCAAATAAAATCCCGTTATTTTTACGAATACCCTA
CACGATTACGACTAACGCCTTTACAATACAAGTATCACTGACCACATTTG
AGTTTGCTGTACAAAATACCGTTAGCGGTGCACTCAACAGCTGAGCGGC
GCTCAAGCTAACCCGCCGATAATGCAGAC
aacaaaaaaagtattaagcaggtagattggcaggcaggtgtaaaatttcggaacacgcacactcttgtgat
tgtgtatgaatgcgaaacggcgtacgctctcgcaaacgctcctacgagtataaaaaccgttctccgtcgcag
caagcagtcagtatctccacagcagcagaggcgacgggaagacaaagcaatctgaattgaatacgtcct
agttttgggtccgtataacaaaaaaatttatagtgcaaagtagctgagataagcgcggcttgacccgggaa
aggcgccagagatgggggcatgcaatataacagtcttattgctggt
CATCATGTTGTGGGTGAGTTATATACGAACACAAGCCGCAAAGATTTCGA
TTATGTTCTATATTTAAACATTTGTATATATTTCATTAGCTACCCCATGGTC
TGTCCATGGGCAATAGCTGCTCGGCATCGGTGCTGGAGGCGCGTAGGT
TCTTCGAGCTGGAAAATGAACAATTGCGAAGGCGTTTCCATGAGGAATTC
CTTTCCGGCTACAACTATAACACCAATGTAACGGAGGCGAATCGCCAGG
CCATGATCGAAGTGTATGCCCGCAATGCGGAACTGAATAAGCGACTCGC
GCAGCAGATAAAGTCCTCCGATTACGTTCAGTCCGAGGATGCGGATATA
CGACGACAGGCCGAGCACCTATCCAAATTGGGTGCATCCGCTCTGAATG
CCGACGACTACCTGGCCCTGCAGAATGCCATCAGTTCGATGCAGACGAA
CTATGCTACCGCCACCGTGTGCTCGTACACCAATCGCAGTGATTGCTCT
CTCACCCTGGAGCCGCACATACAGGAGCGTCTGTCCCATAGCCGTGATC
CTGCCGAACTGGCTTGGTATTGGCGGGAGTGGCACGATAAGTCCGGAA
CTCCCATGCGGCAGAACTTCGCCGAGTATGTGCGACTGACGCGCAAGG
CATCTCAGTTGAATGGTAAGTGATGGACGCCTAGATAACCCCATGTCTGA
CCCAAATCGGGAGAAATCGGTTCGGGCCAGCACAGGGAGAATAGCTTAT
CCACTTGACATTTATCTGTGGTGAAGTACTTGGGTATTTATACCTAATCTC
GGTGTCA---3’

Fig. 1b *Acer*$^{\Delta 168}$ deleted a 329-bp DNA sequences with a forward primer, *Acer* 1-5′, and a reverse primer, *Acer* 1-3′; a 1,400-bp amplification PCR product was anticipated from the wild-type fly.

References

Lin Huan-Wen 林煥雯 (2004). "Angiotensin-converting enzyme related, *Acer* 基因在果蠅心臟發育功能與調控".

Akasaka, T., S. Klinedinst, K. Ocorr, E. L. Bustamante, S. K. Kim and R. Bodmer (2006). "The ATP-sensitive potassium (KATP) channel-encoded dSUR gene is required for Drosophila heart function and is regulated by tinman." Proc Natl Acad Sci U S A **103**(32): 11999-12004.

Arrese, E. L. and J. L. Soulages (2010). "Insect fat body: energy, metabolism, and regulation." Annu Rev Entomol **55**: 207-225.

Azevedo, J., M. A. Garcia-Fernandez, P. Puerta, M. Moreno, M. Desco and J. L. Delcan (1997). "[Dynamic tridimensional echocardiography and evaluation of functional alterations in acute ischemia]." Rev Port Cardiol **16**(11): 913-917.

Azpiazu, N. and M. Frasch (1993). "tinman and bagpipe: two homeo box genes that determine cell fates in the dorsal mesoderm of Drosophila." Genes Dev **7**(7B): 1325-1340.

Bier, E. and R. Bodmer (2004). "Drosophila, an emerging model for cardiac disease." Gene **342**(1): 1-11.

Bodmer, R. (1993). "The gene tinman is required for specification of the heart and visceral muscles in Drosophila." Development **118**(3): 719-729.

Bodmer, R., L. Y. Jan and Y. N. Jan (1990). "A new homeobox-containing gene, msh-2, is transiently expressed early during mesoderm formation of Drosophila." Development **110**(3): 661-669.

Boehm, M. and E. G. Nabel (2002). "Angiotensin-converting enzyme 2--a new cardiac regulator." N Engl J Med **347**(22): 1795-1797.

Bradu, A., L. Ma, J. W. Bloor and A. Podoleanu (2009). "Dual optical

coherence tomography/fluorescence microscopy for monitoring of Drosophila melanogaster larval heart." J Biophotonics **2**(6-7): 380-388.

Brand, A. H. and N. Perrimon (1993). "Targeted gene expression as a means of altering cell fates and generating dominant phenotypes." Development **118**(2): 401-415.

Burrell, L. M., S. B. Harrap, E. Velkoska and S. K. Patel (2013). "The ACE2 gene: its potential as a functional candidate for cardiovascular disease." Clin Sci (Lond) **124**(2): 65-76.

Burrell, L. M., C. I. Johnston, C. Tikellis and M. E. Cooper (2004). "ACE2, a new regulator of the renin-angiotensin system." Trends Endocrinol Metab **15**(4): 166-169.

Cammarato, A., C. M. Dambacher, A. F. Knowles, W. A. Kronert, R. Bodmer, K. Ocorr and S. I. Bernstein (2008). "Myosin transducer mutations differentially affect motor function, myofibril structure, and the performance of skeletal and cardiac muscles." Mol Biol Cell **19**(2): 553-562.

Carhan, A., K. Tang, C. A. Shirras, A. D. Shirras and R. E. Isaac (2011). "Loss of Angiotensin-converting enzyme-related (ACER) peptidase disrupts night-time sleep in adult Drosophila melanogaster." J Exp Biol **214**(Pt 4): 680-686.

Chintapalli, V. R., J. Wang and J. A. Dow (2007). "Using FlyAtlas to identify better Drosophila melanogaster models of human disease." Nat Genet **39**(6): 715-720.

Choma, M. A., S. D. Izatt, R. J. Wessells, R. Bodmer and J. A. Izatt (2006). "Images in cardiovascular medicine: in vivo imaging of the adult Drosophila melanogaster heart with real-time optical coherence

tomography." Circulation **114**(2): e35-36.

Choma, M. A., M. J. Suter, B. J. Vakoc, B. E. Bouma and G. J. Tearney (2010). "Heart wall velocimetry and exogenous contrast-based cardiac flow imaging in Drosophila melanogaster using Doppler optical coherence tomography." J Biomed Opt **15**(5): 056020.

Clark, A. G., M. B. Eisen, et. al. Mauceli and I. MacCallum (2007). "Evolution of genes and genomes on the Drosophila phylogeny." Nature **450**(7167): 203-218.

Coates, D., R. E. Isaac, J. Cotton, R. Siviter, T. A. Williams, A. Shirras, P. Corvol and V. Dive (2000). "Functional conservation of the active sites of human and Drosophila angiotensin I-converting enzyme." Biochemistry **39**(30): 8963-8969.

Coldman, A. J. and J. M. Elwood (1979). "Examining survival data." Can Med Assoc J **121**(8): 1065-1068, 1071.

Crackower, M. A., R. Sarao, G. Y. Oudit, C. Yagil, I. Kozieradzki, S. E. Scanga, A. J. Oliveira-dos-Santos, J. da Costa, L. Zhang, Y. Pei, J. Scholey, C. M. Ferrario, A. S. Manoukian, M. C. Chappell, P. H. Backx, Y. Yagil and J. M. Penninger (2002). "Angiotensin-converting enzyme 2 is an essential regulator of heart function." Nature **417**(6891): 822-828.

Cripps, R. M. and E. N. Olson (2002). "Control of cardiac development by an evolutionarily conserved transcriptional network." Dev Biol **246**(1): 14-28.

Das, P. M., K. Ramachandran, J. vanWert and R. Singal (2004). "Chromatin immunoprecipitation assay." Biotechniques **37**(6): 961-969.

Diop, S. B. and R. Bodmer (2012). "Drosophila as a model to study the genetic mechanisms of obesity-associated heart dysfunction." J Cell Mol

Med **16**(5): 966-971.

Donoghue, M., F. Hsieh, E. Baronas, K. Godbout, M. Gosselin, N. Stagliano, M. Donovan, B. Woolf, K. Robison, R. Jeyaseelan, R. E. Breitbart and S. Acton (2000). "A novel angiotensin-converting enzyme-related carboxypeptidase (ACE2) converts angiotensin I to angiotensin 1-9." Circ Res **87**(5): E1-9.

Donoghue, M., H. Wakimoto, C. T. Maguire, S. Acton, P. Hales, N. Stagliano, V. Fairchild-Huntress, J. Xu, J. N. Lorenz, V. Kadambi, C. I. Berul and R. E. Breitbart (2003). "Heart block, ventricular tachycardia, and sudden death in ACE2 transgenic mice with downregulated connexins." J Mol Cell Cardiol **35**(9): 1043-1053.

Douglas, J. G., M. Romero and U. Hopfer (1990). "Signaling mechanisms coupled to the angiotensin receptor of proximal tubular epithelium." Kidney Int Suppl **30**: S43-47.

Dulcis, D. and R. B. Levine (2005). "Glutamatergic innervation of the heart initiates retrograde contractions in adult Drosophila melanogaster." J Neurosci **25**(2): 271-280.

Ferrario, C. M., J. Jessup, M. C. Chappell, D. B. Averill, K. B. Brosnihan, E. A. Tallant, D. I. Diz and P. E. Gallagher (2005). "Effect of angiotensin-converting enzyme inhibition and angiotensin II receptor blockers on cardiac angiotensin-converting enzyme 2." Circulation **111**(20): 2605-2610.

Ferrario, C. M., J. Jessup, P. E. Gallagher, D. B. Averill, K. B. Brosnihan, E. Ann Tallant, R. D. Smith and M. C. Chappell (2005). "Effects of renin-angiotensin system blockade on renal angiotensin-(1-7) forming enzymes and receptors." Kidney Int **68**(5): 2189-2196.

Ferreira, A. J. and R. A. Santos (2005). "Cardiovascular actions of angiotensin-(1-7)." Braz J Med Biol Res **38**(4): 499-507.

Fink, M., C. Callol-Massot, A. Chu, P. Ruiz-Lozano, J. C. Izpisua Belmonte, W. Giles, R. Bodmer and K. Ocorr (2009). "A new method for detection and quantification of heartbeat parameters in Drosophila, zebrafish, and embryonic mouse hearts." Biotechniques **46**(2): 101-113.

Furberg, C. D., B. M. Psaty, T. A. Manolio, J. M. Gardin, V. E. Smith and P. M. Rautaharju (1994). "Prevalence of atrial fibrillation in elderly subjects (the Cardiovascular Health Study)." Am J Cardiol **74**(3): 236-241.

Gajewski, K., Y. Kim, Y. M. Lee, E. N. Olson and R. A. Schulz (1997). "D-mef2 is a target for Tinman activation during Drosophila heart development." EMBO J **16**(3): 515-522.

Grady, L. (2006). "Random walks for image segmentation." IEEE Trans Pattern Anal Mach Intell **28**(11): 1768-1783.

Guo, S. Y., F. T. Liao, M. T. Su, C. Y. Chang, H. R. Su, J. C. Huang and W. C. Kuo (2013). "Semiautomatic and rapid quantification of heartbeat parameters in Drosophila using optical coherence tomography imaging." J Biomed Opt **18**(2): 26004.

Gurley, S. B., A. Allred, T. H. Le, R. Griffiths, L. Mao, N. Philip, T. A. Haystead, M. Donoghue, R. E. Breitbart, S. L. Acton, H. A. Rockman and T. M. Coffman (2006). "Altered blood pressure responses and normal cardiac phenotype in ACE2-null mice." J Clin Invest **116**(8): 2218-2225.

Han, Z., P. Yi, X. Li and E. N. Olson (2006). "Hand, an evolutionarily conserved bHLH transcription factor required for Drosophila cardiogenesis and hematopoiesis." Development **133**(6): 1175-1182.

Hardoon, D. R., S. Szedmak and J. Shawe-Taylor (2004). "Canonical correlation analysis: an overview with application to learning methods." Neural Comput **16**(12): 2639-2664.

Horiuchi, M., J. Y. Lehtonen and L. Daviet (1999). "Signaling Mechanism of the AT2 Angiotensin II Receptor: Crosstalk between AT1 and AT2 Receptors in Cell Growth." Trends Endocrinol Metab **10**(10): 391-396.

Houard, X., T. A. Williams, A. Michaud, P. Dani, R. E. Isaac, A. D. Shirras, D. Coates and P. Corvol (1998). "The Drosophila melanogaster-related angiotensin-I-converting enzymes Acer and Ance--distinct enzymic characteristics and alternative expression during pupal development." Eur J Biochem **257**(3): 599-606.

Huang, D., E. A. Swanson, C. P. Lin, J. S. Schuman, W. G. Stinson, W. Chang, M. R. Hee, T. Flotte, K. Gregory, C. A. Puliafito and et al. (1991). "Optical coherence tomography." Science **254**(5035): 1178-1181.

Huang, L., D. J. Sexton, K. Skogerson, M. Devlin, R. Smith, I. Sanyal, T. Parry, R. Kent, J. Enright, Q. L. Wu, G. Conley, D. DeOliveira, L. Morganelli, M. Ducar, C. R. Wescott and R. C. Ladner (2003). "Novel peptide inhibitors of angiotensin-converting enzyme 2." J Biol Chem **278**(18): 15532-15540.

Huentelman, M. J., J. L. Grobe, J. Vazquez, J. M. Stewart, A. P. Mecca, M. J. Katovich, C. M. Ferrario and M. K. Raizada (2005). "Protection from angiotensin II-induced cardiac hypertrophy and fibrosis by systemic lentiviral delivery of ACE2 in rats." Exp Physiol **90**(5): 783-790.

Isaac, R. E., R. J. Siviter, P. Stancombe, D. Coates and A. D. Shirras (2000). "Conserved roles for peptidases in the processing of invertebrate

neuropeptides." Biochem Soc Trans **28**(4): 460-464.

Jin, H. Y., B. Song, G. Y. Oudit, S. T. Davidge, H. M. Yu, Y. Y. Jiang, P. J. Gao, D. L. Zhu, G. Ning, Z. Kassiri, J. M. Penninger and J. C. Zhong (2012). "ACE2 deficiency enhances angiotensin II-mediated aortic profilin-1 expression, inflammation and peroxynitrite production." PLoS One **7**(6): e38502.

Jolly, M. P., H. Xue, L. Grady and J. Guehring (2009). "Combining registration and minimum surfaces for the segmentation of the left ventricle in cardiac cine MR images." Med Image Comput Comput Assist Interv **12**(Pt 2): 910-918.

Jose, A. D., F. Stitt and D. Collison (1970). "The effects of exercise and changes in body temperature on the intrinsic heart rate in man." Am Heart J **79**(4): 488-498.

Karram, T., A. Abbasi, S. Keidar, E. Golomb, I. Hochberg, J. Winaver, A. Hoffman and Z. Abassi (2005). "Effects of spironolactone and eprosartan on cardiac remodeling and angiotensin-converting enzyme isoforms in rats with experimental heart failure." Am J Physiol Heart Circ Physiol **289**(4): H1351-1358.

Kaushik, G., A. Fuhrmann, A. Cammarato and A. J. Engler (2011). "In situ mechanical analysis of myofibrillar perturbation and aging on soft, bilayered Drosophila myocardium." Biophys J **101**(11): 2629-2637.

Keidar, S., M. Kaplan and A. Gamliel-Lazarovich (2007). "ACE2 of the heart: From angiotensin I to angiotensin (1-7)." Cardiovasc Res **73**(3): 463-469.

Keidar, S., A. Strizevsky, A. Raz and A. Gamliel-Lazarovich (2007). "ACE2 activity is increased in monocyte-derived macrophages from

prehypertensive subjects." Nephrol Dial Transplant **22**(2): 597-601.

Kim, H. M., D. R. Shin, O. J. Yoo, H. Lee and J. O. Lee (2003). "Crystal structure of Drosophila angiotensin I-converting enzyme bound to captopril and lisinopril." FEBS Lett **538**(1-3): 65-70.

Kim, Y. and M. Nirenberg (1989). "Drosophila NK-homeobox genes." Proc Natl Acad Sci U S A **86**(20): 7716-7720.

Kremser, T., K. Gajewski, R. A. Schulz and R. Renkawitz-Pohl (1999). "Tinman regulates the transcription of the beta3 tubulin gene (betaTub60D) in the dorsal vessel of Drosophila." Dev Biol **216**(1): 327-339.

Kurdi, M., W. C. De Mello and G. W. Booz (2005). "Working outside the system: an update on the unconventional behavior of the renin-angiotensin system components." Int J Biochem Cell Biol **37**(7): 1357-1367.

Lambert, D. W., M. Yarski, F. J. Warner, P. Thornhill, E. T. Parkin, A. I. Smith, N. M. Hooper and A. J. Turner (2005). "Tumor necrosis factor-alpha convertase (ADAM17) mediates regulated ectodomain shedding of the severe-acute respiratory syndrome-coronavirus (SARS-CoV) receptor, angiotensin-converting enzyme-2 (ACE2)." J Biol Chem **280**(34): 30113-30119.

Leckie, B. J. (2005). "Targeting the renin-angiotensin system: what's new?" Curr Med Chem Cardiovasc Hematol Agents **3**(1): 23-32.

Lee, Y. S. and R. W. Carthew (2003). "Making a better RNAi vector for Drosophila: use of intron spacers." Methods **30**(4): 322-329.

Levy, B. I. (2005). "How to explain the differences between renin angiotensin system modulators." Am J Hypertens **18**(9 Pt 2): 134S-141S.

Lijnen, P. J., V. V. Petrov, K. C. Jackson and R. H. Fagard (2001). "Effect of telmisartan on angiotensin II-mediated collagen gel contraction by adult rat cardiac fibroblasts." J Cardiovasc Pharmacol **38**(1): 39-48.

Lockwood, W. K. and R. Bodmer (2002). "The patterns of wingless, decapentaplegic, and tinman position the Drosophila heart." Mech Dev **114**(1-2): 13-26.

Ma, L., A. Bradu, A. G. Podoleanu and J. W. Bloor (2010). "Arrhythmia caused by a Drosophila tropomyosin mutation is revealed using a novel optical coherence tomography instrument." PLoS One **5**(12): e14348.

Manay, S. and A. Yezzi (2003). "Anti-geometric diffusion for adaptive thresholding and fast segmentation." IEEE Trans Image Process **12**(11): 1310-1323.

Monier, B., M. Astier, M. Semeriva and L. Perrin (2005). "Steroid-dependent modification of Hox function drives myocyte reprogramming in the Drosophila heart." Development **132**(23): 5283-5293.

Nishimura, M., K. Ocorr, R. Bodmer and J. Cartry (2011). "Drosophila as a model to study cardiac aging." Exp Gerontol **46**(5): 326-330.

Ocorr, K., T. Akasaka and R. Bodmer (2007). "Age-related cardiac disease model of Drosophila." Mech Ageing Dev **128**(1): 112-116.

Ocorr, K., M. Fink, A. Cammarato, S. Bernstein and R. Bodmer (2009). "Semi-automated Optical Heartbeat Analysis of small hearts." J Vis Exp(31).

Ocorr, K., N. L. Reeves, R. J. Wessells, M. Fink, H. S. Chen, T. Akasaka, S. Yasuda, J. M. Metzger, W. Giles, J. W. Posakony and R. Bodmer (2007). "KCNQ potassium channel mutations cause cardiac arrhythmias

in Drosophila that mimic the effects of aging." Proc Natl Acad Sci U S A **104**(10): 3943-3948.

Oudit, G. Y., Z. Kassiri, M. P. Patel, M. Chappell, J. Butany, P. H. Backx, R. G. Tsushima, J. W. Scholey, R. Khokha and J. M. Penninger (2007). "Angiotensin II-mediated oxidative stress and inflammation mediate the age-dependent cardiomyopathy in ACE2 null mice." Cardiovasc Res **75**(1): 29-39.

Paternostro, G., C. Vignola, D. U. Bartsch, J. H. Omens, A. D. McCulloch and J. C. Reed (2001). "Age-associated cardiac dysfunction in Drosophila melanogaster." Circ Res **88**(10): 1053-1058.

Pena Silva, R. A., Y. Chu, J. D. Miller, I. J. Mitchell, J. M. Penninger, F. M. Faraci and D. D. Heistad (2012). "Impact of ACE2 deficiency and oxidative stress on cerebrovascular function with aging." Stroke **43**(12): 3358-3363.

Qian, L. and R. Bodmer (2012). "Probing the polygenic basis of cardiomyopathies in Drosophila." J Cell Mol Med **16**(5): 972-977.

Quan, G. X., K. Mita, K. Okano, T. Shimada, N. Ugajin, Z. Xia, N. Goto, E. Kanke and H. Kawasaki (2001). "Isolation and expression of the ecdysteroid-inducible angiotensin-converting enzyme-related gene in wing discs of Bombyx mori." Insect Biochem Mol Biol **31**(1): 97-103.

Raizada, M. K. and A. J. Ferreira (2007). "ACE2: a new target for cardiovascular disease therapeutics." J Cardiovasc Pharmacol **50**(2): 112-119.

Reim, I. and M. Frasch (2005). "The Dorsocross T-box genes are key components of the regulatory network controlling early cardiogenesis in Drosophila." Development **132**(22): 4911-4925.

Riviere, G., A. Michaud, C. Breton, G. VanCamp, C. Laborie, M. Enache, J. Lesage, S. Deloof, P. Corvol and D. Vieau (2005). "Angiotensin-converting enzyme 2 (ACE2) and ACE activities display tissue-specific sensitivity to undernutrition-programmed hypertension in the adult rat." Hypertension **46**(5): 1169-1174.

Roma, G. C., O. C. Bueno and M. I. Camargo-Mathias (2010). "Morpho-physiological analysis of the insect fat body: a review." Micron **41**(5): 395-401.

Roth, D. M., J. S. Swaney, N. D. Dalton, E. A. Gilpin and J. Ross, Jr. (2002). "Impact of anesthesia on cardiac function during echocardiography in mice." Am J Physiol Heart Circ Physiol **282**(6): H2134-2140.

Rusch, J. and M. Levine (1997). "Regulation of a dpp target gene in the Drosophila embryo." Development **124**(2): 303-311.

Ryan, K. M., J. D. Hendren, L. A. Helander and R. M. Cripps (2007). "The NK homeodomain transcription factor Tinman is a direct activator of seven-up in the Drosophila dorsal vessel." Dev Biol **302**(2): 694-702.

Santos, P. C., J. E. Krieger and A. C. Pereira (2012). "Renin-angiotensin system, hypertension, and chronic kidney disease: pharmacogenetic implications." J Pharmacol Sci **120**(2): 77-88.

Schelling, P., H. Fischer and D. Ganten (1991). "Angiotensin and cell growth: a link to cardiovascular hypertrophy?" J Hypertens **9**(1): 3-15.

Shapiro, L. G. and R. M. Haralick (1985). "A metric for comparing relational descriptions." IEEE Trans Pattern Anal Mach Intell **7**(1): 90-94.

Siviter, R. J., R. J. Nachman, M. P. Dani, J. N. Keen, A. D. Shirras and R.

E. Isaac (2002). "Peptidyl dipeptidases (Ance and Acer) of Drosophila melanogaster: major differences in the substrate specificity of two homologs of human angiotensin I-converting enzyme." Peptides **23**(11): 2025-2034.

Slama, K. (2012). "A new look at the comparative physiology of insect and human hearts." J Insect Physiol **58**(8): 1072-1081.

Strobel, J. S., A. E. Epstein, R. C. Bourge, J. K. Kirklin and G. N. Kay (1999). "Nonpharmacologic validation of the intrinsic heart rate in cardiac transplant recipients." J Interv Card Electrophysiol **3**(1): 15-18.

Tatei, K., H. Cai, Y. T. Ip and M. Levine (1995). "Race: a Drosophila homologue of the angiotensin converting enzyme." Mech Dev **51**(2-3): 157-168.

Taylor, C. A., D. Coates and A. D. Shirras (1996). "The Acer gene of Drosophila codes for an angiotensin-converting enzyme homologue." Gene **181**(1-2): 191-197.

Thom, T., P. Wolf et al. (2006). "Heart disease and stroke statistics--2006 update: a report from the American Heart Association Statistics Committee and Stroke Statistics Subcommittee." Circulation **113**(6): e85-151.

Tian, X., D. Hansen, T. Schedl and J. B. Skeath (2004). "Epsin potentiates Notch pathway activity in Drosophila and C. elegans." Development **131**(23): 5807-5815.

Tipnis, S. R., N. M. Hooper, R. Hyde, E. Karran, G. Christie and A. J. Turner (2000). "A human homolog of angiotensin-converting enzyme. Cloning and functional expression as a captopril-insensitive carboxypeptidase." J Biol Chem **275**(43): 33238-33243.

Tobias, O. J. and R. Seara (2002). "Image segmentation by histogram thresholding using fuzzy sets." IEEE Trans Image Process **11**(12): 1457-1465.

Tokusumi, T., M. Russell, K. Gajewski, N. Fossett and R. A. Schulz (2007). "U-shaped protein domains required for repression of cardiac gene expression in Drosophila." Differentiation **75**(2): 166-174.

Touyz, R. M. (2003). "Reactive oxygen species in vascular biology: role in arterial hypertension." Expert Rev Cardiovasc Ther **1**(1): 91-106.

Tsai, M. T., F. Y. Chang, C. K. Lee, T. T. Chi, K. M. Yang, L. Y. Lin, J. T. Wu and C. C. Yang (2011). "Observations of cardiac beating behaviors of wild-type and mutant Drosophilae with optical coherence tomography." J Biophotonics **4**(9): 610-618.

Vaughan, D. E. (2001). "Angiotensin, fibrinolysis, and vascular homeostasis." Am J Cardiol **87**(8A): 18C-24C.

Vickers, C., P. Hales, V. Kaushik, L. Dick, J. Gavin, J. Tang, K. Godbout, T. Parsons, E. Baronas, F. Hsieh, S. Acton, M. Patane, A. Nichols and P. Tummino (2002). "Hydrolysis of biological peptides by human angiotensin-converting enzyme-related carboxypeptidase." J Biol Chem **277**(17): 14838-14843.

Volpe, M. (2012). "Preventing cardiovascular events with angiotensin II receptor blockers: a closer look at telmisartan and valsartan." Expert Rev Cardiovasc Ther **10**(8): 1061-1072.

Wang, J., Y. Tao, I. Reim, K. Gajewski, M. Frasch and R. A. Schulz (2005). "Expression, regulation, and requirement of the toll transmembrane protein during dorsal vessel formation in Drosophila melanogaster." Mol Cell Biol **25**(10): 4200-4210.

Wang, W., S. Bodiga, S. K. Das, J. Lo, V. Patel and G. Y. Oudit (2012). "Role of ACE2 in diastolic and systolic heart failure." Heart Fail Rev **17**(4-5): 683-691.

Warner, F. J., A. I. Smith, N. M. Hooper and A. J. Turner (2004). "Angiotensin-converting enzyme-2: a molecular and cellular perspective." Cell Mol Life Sci **61**(21): 2704-2713.

Wessells, R. J. and R. Bodmer (2004). "Screening assays for heart function mutants in Drosophila." Biotechniques **37**(1): 58-60, 62, 64 passim.

Wessells, R. J., E. Fitzgerald, J. R. Cypser, M. Tatar and R. Bodmer (2004). "Insulin regulation of heart function in aging fruit flies." Nat Genet **36**(12): 1275-1281.

Whaley-Connell, A. and J. R. Sowers (2012). "Oxidative stress in the cardiorenal metabolic syndrome." Curr Hypertens Rep **14**(4): 360-365.

Williams, T. A., S. Danilov, F. Alhenc-Gelas and F. Soubrier (1996). "A study of chimeras constructed with the two domains of angiotensin I-converting enzyme." Biochem Pharmacol **51**(1): 11-14.

Wolf, M. J., H. Amrein, J. A. Izatt, M. A. Choma, M. C. Reedy and H. A. Rockman (2006). "Drosophila as a model for the identification of genes causing adult human heart disease." Proc Natl Acad Sci U S A **103**(5): 1394-1399.

Xia, H., S. Suda, S. Bindom, Y. Feng, S. B. Gurley, D. Seth, L. G. Navar and E. Lazartigues (2011). "ACE2-mediated reduction of oxidative stress in the central nervous system is associated with improvement of autonomic function." PLoS One **6**(7): e22682.

Yamamoto, K., M. Ohishi, T. Katsuya, N. Ito, M. Ikushima, M. Kaibe, Y.

Tatara, A. Shiota, S. Sugano, S. Takeda, H. Rakugi and T. Ogihara (2006). "Deletion of angiotensin-converting enzyme 2 accelerates pressure overload-induced cardiac dysfunction by increasing local angiotensin II." Hypertension **47**(4): 718-726.

Zaffran, S., I. Reim, L. Qian, P. C. Lo, R. Bodmer and M. Frasch (2006). "Cardioblast-intrinsic Tinman activity controls proper diversification and differentiation of myocardial cells in Drosophila." Development **133**(20): 4073-4083.